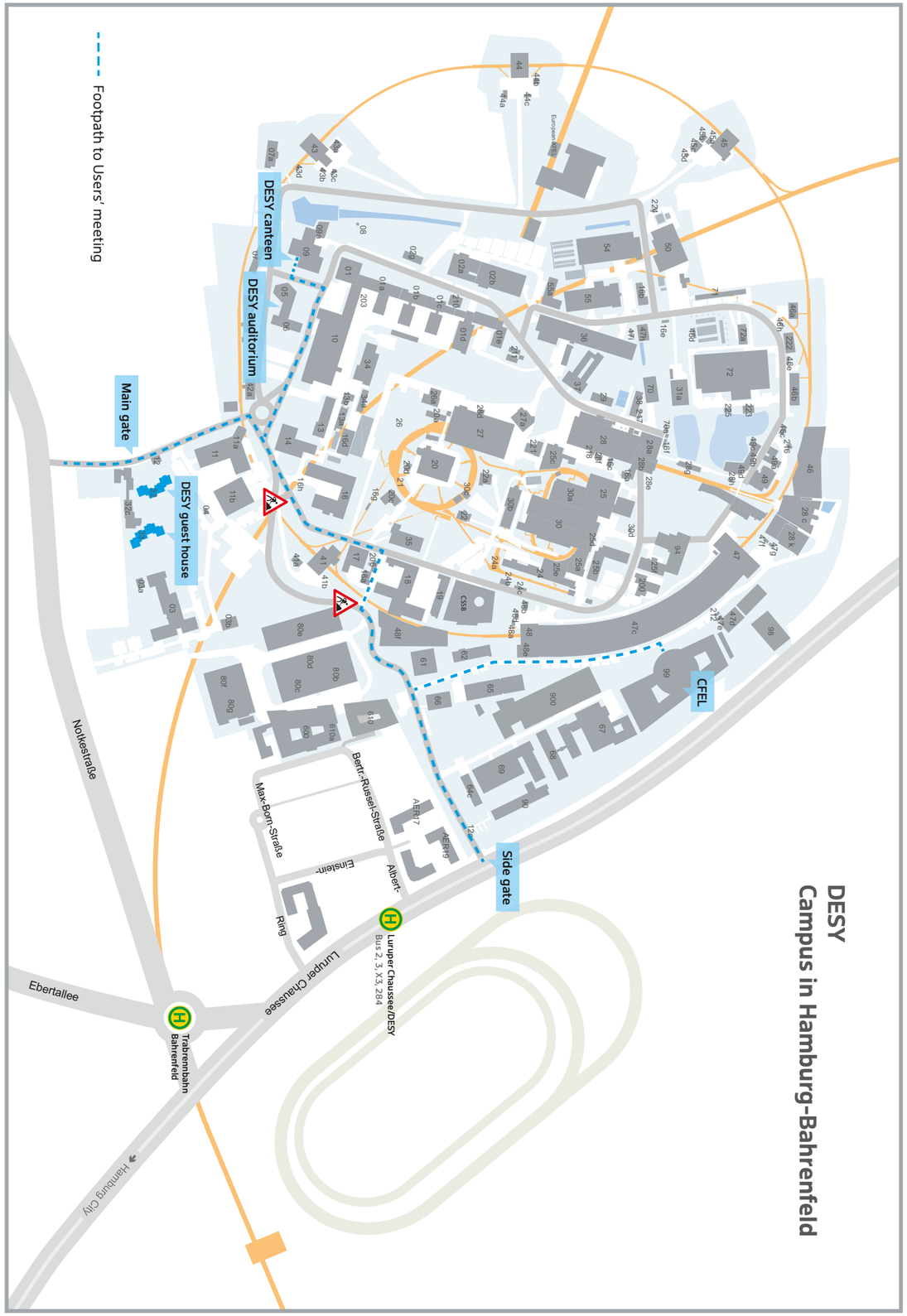

DESY Photon Science Users' Meeting 2026
European XFEL Users' Meeting 2026

Jointly organized Users' Meeting of
DESY Photon Science and European XFEL

DESY Photon Science Users' Meeting 2026
European XFEL Users' Meeting 2026
in Hamburg, Germany
DESY Auditorium (Bldg. 5) & CFEL Foyer (Bldg. 99)

Friday, Januar 23: Satellite Workshops		Location
10:00 – 17:00	European XFEL | European XFEL data workshop	Zoom
Monday, Januar 26: Satellite Workshops		
several days	DESY, European XFEL, EMBL | MX satellite meeting	Visit Website
09:00	DESY | Temporally Coherent Synchrotron Light Sources	DESY, Bldg. 1b, Seminar room 4ab
12:00	DESY, European XFEL | Prospects of Momentum Microscopy at PETRA III, FLASH, and European XFEL	European XFEL
12:30	European XFEL | Satellite Workshop on Photon Diagnostics (XPD)	European XFEL, Lighthouse Auditorium
14:30 – 18:00	DESY | Community proposal at the seeded FLASH1	DESY, Bldg. 28c, FLASH Seminar room

Tuesday, January 27: European XFEL Users' Meeting
(DESY Campus, Bldg. 5, Audithorium)

		Speaker	Affiliation
08:00 – 09:00	**Registration**		
09:00 – 10:55	Opening Session	Chair: Serguei Molodtsov (European XFEL)	
09:00	Welcome/Opening	Federico Boscherini	CNR, Trieste
09:05	European XFEL: Current status and future developments	Thomas Feurer	European XFEL
09:45	First Lasing of an XFEL Oscillator	Harald Sinn	European XFEL
10:15	Update from the European Synchrotron and FEL User Organization (ESUO)	Bridget Murphy	Uni Kiel
10:25	European XFEL User Organization and Young Scientist Award	Marc Simon/ Friedrich Roth	CNRS-European XFEL IRL / TU Freiberg
10:35	Award talk by the winner of the Young Scientist Award	To be announced	
10:55 – 11:25	**Coffee break**		
11:25 – 12:55	Science session I	Chair: Raphael Jay (Univ. Uppsala)	
11:25	Operando Multiscale X-ray Imaging of Defects & Alloying at XFELs in LPBF	Leora Dresselhaus-Marais	SLAC
11:55	Time-resolved RIXS of the laser induced insulator-to-metal transition in $NdNiO_3$	Thorsten Schmitt	PSI
12:25	Ultrafast dynamics of photoexcited states in cerium oxide by pump-probe Ce L3-edge XANES and EXAFS	Paola Luches	CNR-NANO, Modena
12:55 – 14:10	**Lunch break**		
14:10 – 15:40	Science session II	Chair: Volha Chukhutsina (VU Amsterdam)	
14:10	Structure of liquid carbon and mixtures of light elements at high pressures	Dominik Kraus	Uni Rostock
14:40	Atomic and molecular quantum dynamics at FELs, from stochastic temporal correlations at FLASH to attosecond double pulses at	Thomas Pfeifer	MPIK, Heidelberg
15:10	Investigating protein anomalous diffusion with coherent X-rays	Anita Girelli	Uni Stockholm
From 15:55	**Bus transfer from DESY to European XFEL, Schenefeld campus**		
16:40 – 19:00	**Poster session I – European XFEL** **(European XFEL, Schenefeld campus)**		
19:00 – 22:00	**Get together** **(Lighthouse visitor center, European XFEL, Schenefeld campus)**		

Wednesday, Januar 28: Satellite Workshops

9:00 – 12:00	DESY | Industry Satellite Meeting 2026: Connecting Science, Services & Standards	DESY, Bldg. 610, Ground floor
9:00 – 12:00	European XFEL | Twin bunch mode operation for experiments at HED-HIBEF	European XFEL, Bldg. XHO, Lounge
9:00 – 12:00	DESY | XPCS at PETRA IV: Present Status and Future Upgrade Plans for Coherent Application Beamline P10	DESY, Bldg. 28c, FLASH Seminar room
9:00 – 18:30	European XFEL | Pump-Probe lasers 2030+	European XFEL, Bldg. XHQ, E1.173
9:30 – 16:30	DESY | SAXS/WAXS/GISAXS @ DESY	DESY, Bldg. 15, Auditorium
11:00 – 15:30	DESY | DAPHNE4NFDI: Making Data FAIR and AI-Ready	DESY, Bldg. 1b, Seminar room 4ab
12:30 – 16:30	Hereon | Helmholtz-Zentrum Hereon GEMS Outstation: Materials Research and High-Resolution Imaging	DESY, Bldg. 94, CXNS Seminar room 01.104
13:00 – 18:00	European XFEL | HED-HIBEF satellite meeting: Instrument updates and science highlights	European XFEL, Visitor Centre Lighthouse
13:00 – 16:30	DESY | 16th Workshop on X-Ray Nano-Imaging of Biological and Chemical Systems at PETRA III	DESY, Bldg. 28c, FLASH Seminar room

Wednesday, January 28: DESY Photon Science Users' Meeting (FLASH) & Joint Session
(DESY Campus, Bldg. 5, Audithorium)

		Speaker	Affiliation
08:30	**Registration**		
		Chairperson: E. Plönjes (DESY)	
09:00	Welcome	Beate Heinemann	DESY
09:05	Welcome to the FEL Session	Britta Redlich	DESY
09:20	FLASH status und strategy	Markus Gühr	DESY
09:50	FLASH 2020+ Activties - Update	Lucas Schaper	DESY
10:20 – 11:00	**Coffee break**		
		Chairperson: K. Tiedtke (DESY)	
11:00	Nitrogen K-edge Time-Resolved XAS for Probing Photoinduced Dynamics in Azobenzene	Rebecca Ingle	University College London
11:20	Femtosecond charge and spin dynamics in a Co50Pt50 alloy	Martin Pavelka	Uppsala University
11:40	Dynamics of CO Photooxidation to CO_2 on Rutile(110) and Anatase(101) Surfaces	Heshmat Noei	DESY
12:00	Melting, Bubblelike Expansion, and Explosion of Superheated Plasmonic Nanoparticles	Simon Dold	European XFEL
12:20 – 14:00	**Lunch break**		
14:00 – 16:00	**Synergies between FLASH and EuXFEL (Jointly organised session)**		
		Chairperson: F. Roth (TU Freiberg)	
14:00	Visualizing the Three-Dimensional Arrangement of Hydrogen Atoms in Organic Molecules by Coulomb Explosion Imaging	Alice Green	University of Edinburgh
14:20	Electronic Molecular Movies with FELs: The Ultrafast Dynamics of 2-thiouracil	Fabiano Lever	DESY
14:40	Soft-X-ray ARPES from Static to Out-of-Equilibrium Electronic States	Vladimir Strokov	PSI Villigen
15:00	Synergistic ultrafast k-microscopy at FLASH and EuXFEL	Kai Rossnagel	CAU Kiel, DESY
15:30 – 19:00	**POSTER SESSION II and Vendor exhibition** **(DESY campus, Bldg. 99, CFEL)**		
19:00 – 22:00	**Get together** **(DESY canteen, Bldg. 9)**		

Thursday, 29 January: DESY Photon Science Users' Meeting (PETRA III) & Satellite Workshops
(DESY Campus, Bldg. 5, Audithorium)

		Speaker	Affiliation
08:30	**Registration**		
		Chairperson: S. Techert (DESY, Univ. Göttingen)	
09:00	Welcome and Overview DESY Photon Science	Britta Redlich	DESY
09:30	PETRA III Status	Christian Schroer	DESY, UHH
10:00	Research with Photons – Light for the Future: News from the KFS (Committee Research with Synchrotron Radiation)	Christian Gutt (KFS Chair)	Uni Siegen (Germany)
10:15 – 11:00	**Coffee break**		
		Chairperson: B. Redlich (DESY)	
11:00	PETRA IV Project Status	Harald Reichert	DESY
11:30	PETRA IV Experimental Program	Kai Bagschik	DESY
12:00	PETRA IV Beamlines with a focus on Imaging	Christian Schroer	DESY, UHH
12:15	PETRA IV Beamlines with a focus on Spectroscopy	Hans-Christian Wille	DESY
12:30	PETRA IV Beamlines with a focus on Scattering and Diffraction	Oliver Seeck	DESY
12:45 – 14:10	**Lunch break**		
		Chairperson: S. Roth (DESY, KTH Stockholm)	
14:10	Report of the 'DESY Photon Science User Committee' (DPS-UC) Results of the DPS-UC election	Peter Müller-Buschbaum	TU München
14:20	DESY Photon Science User Award 2025 (ceremony and talk)	Heinz Graafsma (Chair Award commit.)	DESY
14:30	X-ray Vision - revealing hidden structures with chemical imaging	Stephen Price	Finden Ltd./ University of Sheffield
14:50	Macromolecular assemblies in realistic solution conditions	Uri Raviv	Hebrew University of Jerusalem
15:10	Using X-rays to rejuvenate glasses	Giulio Monaco	Univ. Padova
15:30	Quantum technologies meet functional materials: What X-rays can reveal	Martina Müller	Uni Konstanz
15:50	Structural features of lignin based thermosets	Mats Johansson	KTH Stockholm
16:10	Catching Matter in the Act: Real-Time Observation of Phase Transformations at Conditions Approaching 1 Mbar and 5000 K	Emma Ehrenreich-Petersen	DESY Hamburg
15:30 – 19:00	**POSTER SESSION III and Vendor exhibition** **(DESY Campus, CFEL, Bldg. 99)**		

Friday, Januar 30: Satellite Workshops

9:00 – 12:00	Enhancing UX in X-ray Optics: Simulations including AI-driven Applications (second day)	European XFEL

ABSTRACTS

Operando Multiscale X-ray Imaging of Defects & Alloying at XFELs in LPBF

L. Dresselhaus-Marais[1]

[1] *Stanford University, Department of Materials Science & Engineering, Stanford, USA*

E-mail: leoradm@stanford.edu

Additive manufacturing (AM) is transforming manufacturing today, with seemingly limitless constraints on shapes and even local composition/properties. Laser powder-bed fusion (LPBF) is one the most used metal AM technique that today enables new design paradigms for metals manufacturing by using a laser to melt and print parts layer by layer. Today's deployment of LPBF to enhance the strength-to-weight ratios that determine the electricity load of most technologies is limited by the variability in defects and structural properties from printed parts, arising from poorly-understood defects at many scales. My group has developed new *operando* X-ray microscopes at X-ray free electron lasers (XFELs) that allow us to advance current understanding of LPBF. We developed the first multiscale X-ray microscopes for LPBF, where our simultaneous sub-μm and mm-scale views of the dynamics can offer key insights into the turbulent fluid dynamics and solidification of the process. Developing the instrumentation, design/simulation software, and analysis methods to process the results, our femtosecond (10^{-15} s) resolution images have now begun to caputre MHz-timescale views of unique processes. I will share the models we are now building from this work to understand in-situ alloying of dissimilar metals during the print. This new capability enabled by the European XFEL now offers unique scientific opportunities for advanced metallurgy and manufacturing science.

Time-resolved RIXS of the laser induced insulator-to-metal transition in $NdNiO_3$

Thorsten Schmitt[1]

[1] *Paul Scherrer Institut, Center for Photon Science, Villigen PSI, Switzerland*

E-mail: thorsten.schmitt@psi.ch

We have studied the ultrafast dynamics of the breathing-distortion in the photo-induced insulator-transition transition (IMT) in $NdNiO_3$ in a pump-probe experiment utilizing RIXS at the Ni L_3-edge as the probe after pumping the material by light pulses across the insulating gap. The breathing-distortion in $NdNiO_3$ is followed by measuring the dd-orbital excitations characteristic for the ligand field environment associated with the NiO_6 octahedra, which evolve across the temperature-induced IMT from the insulating phase with alternating Ni site environments (corresponding to Ni $3d^8$ and Ni $3d^8\underline{L}^2$ electronic configurations with $\underline{L}$ = hole in O2p ligand orbital) to an uniform Ni site environment (with an Ni $3d^8\underline{L}$ valence configuration) in the metallic phase. The difference in the dd-excitations in the insulating state is due to the breathing distortion of alternating compressed or expanded NiO6 octahedra. By pumping the sample with an ultrafast laser pulse of 800 nm wavelength, we suppressed the antiferromagnetic insulating phase and transiently excite the electronic system to the metallic paramagnetic phase. The shape and intensity of the dd-orbital excitations allow monitoring the time evolution of the breathing-distortion and the dynamics of the charge gap after the photoexcitation. We followed the subsequent suppression and recovery of the breathing-distortion along with the collapse of the insulating charge gap by measuring shape and intensity of the dd-orbital and electron-hole pair excitations as a function of the delay between 800 nm pump and RIXS probe pulses.

Ultrafast dynamics of photoexcited states in cerium oxide by pump-probe Ce L_3-edge XANES and EXAFS

P. Luches[1]

[1] *Istituto Nanoscienze, Consiglio Nazionale delle Ricerche, Modena, Italy*

E-mail: paola.luches@nano.cnr.it

Pump-probe X-ray spectroscopies provide element-specific insights into the ultrafast processes triggered by photoexcitation in photocatalysts, providing insights essential for a rational optimization of their efficiency.
Cerium oxide is widely used as a catalyst and photocatalyst due to its ability to undergo reversible Ce^{3+}/Ce^{4+} redox transitions, which enable oxygen vacancy formation and annihilation.
The photoexcitation dynamics in CeO_2 are investigated using ultrafast pump-probe X-ray near-edge spectroscopy (XANES) and extended X-ray absorption fine structure (EXAFS) at the Ce L_3 edge at the FXE instrument, simultaneously probing the ultrafast electronic and local atomic structure modifications [1]. Transient XANES analysis shows that, within the first few tens of fs, the electronic structure undergoes modifications that are compatible with a transient occupation of Ce 4f states. Within approximately 500 fs, the electronic structure partially relaxes to a metastable photoexcited state with a lifetime on the order of hundreds of picoseconds. Transient EXAFS analysis reveals a structural distortion of about 0.14 Å in the first O coordination shell around the excited Ce atom, occurring on the same timescale as the partial relaxation of the electronic structure. This correlated electronic-structural response is consistent with the formation of a photoinduced small-polaron state.
Constrained density functional theory simulations further support this interpretation, showing that the localization of the excited electron on a Ce atom induces an expansion of the neighboring O ions, with a magnitude in agreement with the experimental value.

References

[1] S. Pelatti, E. Spurio, D. Catone, P. O'Keeffe, S. Turchini, G. Ammirati, F. Paleari, D. Varsano, S. Benedetti, A. di Bona, S. D'Addato, Y. Jiang, P. Zalden, Y. Uemura, H. Wang, D. Vinci, X. Huang, F. Lima, M. Biednov, D. Khakhulin, C.J. Milne, F. Boscherini, P. Luches, Ultrafast Dynamics of Electronic and Structural Modifications Induced by Photoexcitation in Cerium Oxide, Adv. Electron. Mater., 11, e00429 (2025).

Structure of liquid carbon and mixtures of light elements at high pressures

D. Kraus[1]

[1] *University of Rostock, Institute of Physics, Rostock, Germany*

Helmholtz-Zentrum Dresden-Rossendorf, Institute of Radiation Physics, Dresden, Germany

E-mail: dominik.kraus@uni-rostockde.de

I will present our latest results on in situ diagnostics of phase transitions and chemical reactions of light elements such as carbon, hydrocarbons and water at extreme pressures and temperatures. Outstanding results include elucidating the structure of liquid carbon [1] and the observation of a mixed close-packed structure in superionic water [2]. Overall, combining X-ray free electron lasers with the new generation of rep-rated high-energy drive lasers allows for high energy density science studies of unprecedented quality and for using novel photon-hungry methodologies with great prospectives for revolutionary insights for planetary physics, inertial fusion energy, and other applications during the next decade [3].

This presentation is on behalf of the collaborations for the EuXFEL experiments 2740, 4463, and 6656.

References

[1] D. Kraus et al., The structure of liquid carbon elucidated by in situ X-ray diffraction**,** Nature **642**, 351-355 (2025)

[2] L. Andriambariarijaona et al., Observation of a mixed close-packed structure in superionic water, Nature Communications (2025). https://doi.org/10.1038/s41467-025-67063-2

[3] D. Kraus et al., Warm dense matter studies with X-ray free-electron lasers**,** Nature Reviews Physics **8**, 27-39 (2026)

Atomic and molecular quantum dynamics at FELs, from stochastic temporal correlations at FLASH to attosecond double pulses at EuXFEL

Thomas Pfeifer

Max-Planck-Institut für Kernphysik (MPIK), Heidelberg, Germany

E-mail: thomas.pfeifer@mpi-hd.mpg.de

To resolve ultrafast events, we need controlled events that are shorter than the delay between the events. Likewise, to resolve closely-spaced spectral lines, we need to achieve spectrometer resolutions better than their spacing. These statements appear correct, at first.

Here, we will shed light on this common knowledge, statistically structured light to be more precise.

The stochastic nature of free-electron laser (FEL) pulses, obtained from self-amplified spontaneous emission (SASE) was originally considered a nuisance, as every shot is a different pulse with a uniquely shaped time-dependent electric field, making comparisons to theory difficult, especially in the absence of online diagnostic measurement tools that record the temporal or spectral structure of each individual FEL pulse.

Starting from early experiments at the extreme-ultraviolet (XUV) FEL FLASH at DESY, we find that by using correlations in statistically structured SASE FEL pulses, the temporal resolution can be substantially increased. Time-dependent motion, structural dynamics, shorter than the FEL pulse duration are resolved, as demonstrated for the example of vibrational wavepackets in the D_2 molecular ion, observed by ion coincidence spectroscopy with a reaction microscope (ReMi) in an XUV-pump–XUV-probe experiment [1].

From a "single-pulse" transmission spectroscopy experiment at EuXFEL, we see how correlations (this time not within the SASE pulses, but) within the physical interaction process itself (X-ray simulated Raman) can be harnessed (in a manner akin to super-resolution microscopy) to resolve spectral structures (a fine-structure splitting in Ne on the 100-meV level) that would otherwise appear only as a broadening in the (0.2 eV) resolution of an x-ray spectrometer [2].

Finally, we look into the current status of our recent attosecond-pump–attosecond-probe experiment conducted at EuXFEL, with the aim to observe, understand, and control electron charge migration in the chemically important carboxyl group of organic acids. Making use of a recently established attosecond double-pulse operating regime at EuXFEL, in particular at closely spaced (mutually overlapping) spectra for pump and probe pulses, we uncover spectral interference structures that encode the time delay of the otherwise stochastically varying SASE pulses. Using post sorting based on shot-to-shot spectral diagnostics, we uncover transient changes of characteristic x-ray absorption below the oxygen K edge, encoding the motion of electrons in the vicinity of the two chemically distinct oxygen atoms in the COOH carboxy group [3].

References

[1] Yuhei Jiang *et al.* PRA ***81****, 051402(R) (2010),* Kristina Meyer *et al.* PRL **108**, 098302 (2012)

[2] Kai Li *et al.* Nature **643**, 662–668 (2025)

[3] in preparation

Investigating protein anomalous diffusion with coherent X-rays

Anita Girelli[1]

[1] *Stockholm University, Stockholm, Sweden*

E-mail: anita.girelli@fysik.su.se

Understanding protein motion under crowded conditions is essential for predicting reaction kinetics and macromolecular transport in the cellular cytoplasm. At molecular length scales, protein dynamics are governed by a subtle interplay between hydrodynamic coupling and direct interparticle interactions, yet experimental access to the relevant time and length scales has remained limited.

Here, we exploit megahertz X-ray Photon Correlation Spectroscopy (MHz-XPCS) at the European X-ray Free Electron Laser (EuXFEL), using the correlation-before-aggregation approach previously developed [1], to probe collective ferritin diffusion on microsecond time scales and nanometer length scales [2]. At elevated protein concentrations, we observe a clear deviation from simple Brownian motion, manifested as a non-exponential decay of the intensity autocorrelation function. This anomalous behavior signals the emergence of cage-trapping between the short-time and long-time diffusion regimes.

By combining the experimental data with modeling based on the δγ-theory for hydrodynamically interacting colloidal spheres, we reproduce the measured diffusion coefficients by introducing a scaling factor associated with direct protein interactions. Our results provide direct experimental evidence of cage effects and long-time diffusion in crowded protein solutions, demonstrating the capability of EuXFEL MHz-XPCS to access collective biomolecular dynamics beyond the short-time limit. These findings have broader implications for understanding intracellular transport and for optimizing ferritin-based nanomedical applications, where diffusion often represents the rate-limiting step.

References

[1] Reiser, M. et al. Resolving molecular diffusion and aggregation of antibody proteins with megahertz X-ray free-electron laser pulses. Nat. Commun. 13, 5528 (2022).

[2] Girelli, A. et al. Coherent X-rays reveal anomalous molecular diffusion and cage effects in crowded protein solutions. Nat. Commun. 16, 10814 (2025).

Nitrogen K-edge Time-Resolved XAS for Probing Photoinduced

Rebecca Ingle

University College London

Azobenzene is often considered the classic example of a photoswitch, undergoing photoisomerization resulting in a significant photochromic shift. Good photoswitching fatigue resistance and selective wavelength control over the forward and backswitching processes have made azobenzene-based motifs ubiquitous in molecular switching applications. However, there have been a relatively limited number of experimental ultrafast spectroscopies studies on isolated azobenzene. Using time-resolved X-ray absorption spectroscopy (TR-XAS) at the nitrogen K-edge, we demonstrate how the excellent sensitivity of TR-XAS to states of different electronic character and site-specific probing capabilities can be used to map the photoinduced dynamics across multiple electronic states as well as changes in the nuclear configuration.

Femtosecond charge and spin dynamics in a Co50Pt50 alloy

Martin Pavelka

Uppsala University

The investigation of ultrafast demagnetization dynamics in multi-element magnetic systems is critical for understanding spin transfer mechanisms, yet it requires experimental tools that combine femtosecond temporal resolution with element-specific magnetic sensitivity [1]. This talk presents the commissioning of a new APPLE-III helical afterburner undulator at the FLASH2 free-electron laser facility, which enables the generation of ultrashort soft x-ray pulses with a degree of circular polarization close to 100% in the range of the $3d$ transition metal L-edges [2, 3]. We characterized the polarization purity using photoelectron spectroscopy and demonstrated the capability for time-resolved X-ray Magnetic Circular Dichroism (XMCD) with an effective temporal resolution of less than 270 fs [2]. Leveraging this new capability, we investigated the femtosecond charge and spin dynamics of a Co${*50}$Pt${50}$ alloy at the Co L_3-edge [3]. By simultaneously monitoring transient changes in the electronic structure via X-ray Absorption Spectroscopy (XAS) and the magnetic order via XMCD, we observed distinctive electronic and magnetic recovery timescales. Furthermore, a comparison with previous studies on CoPd systems [1] revealed that CoPt demagnetizes significantly more efficiently, achieving demagnetization at substantially lower optical pump fluences. We attribute this enhanced demagnetization efficiency to the stronger spin-orbit coupling in the $5d$ element Platinum compared to the $4d$ element Palladium, which facilitates efficient spin-flip scattering processes.

[1] Le Guyader, L. et al. State-resolved ultrafast charge and spin dynamics in [Co/Pd] multilayers. Appl. Phys. Lett. 120, 032401 (2022).

[2] Marotzke, S. et al. First experiments with ultrashort, circularly polarized soft x-ray pulses at FLASH2. Structural Dynamics 12, 034301 (2025).

[3] Pavelka, M. et al. Femtosecond charge and spin dynamics in a Co50Pt50 alloy. Structural Dynamics 12, 024303 (2025).

Dynamics of CO Photooxidation to CO_2 on Rutile(110) and Anatase(101) Surfaces

Heshmat Noei

An acute understanding of photocatalytic reaction dynamics on metal oxides is crucial for the efficient development of technology used for self-cleaning surfaces and for air and water purification. By utilizing femtosecond X-ray laser pulses synchronized with an optical laser (1.6 eV) at FLASH in Hamburg we were able to directly follow the reaction dynamics during photocatalysis at the surface of anatase TiO_2(101) and rutile TiO_2(110) for $CO/O_2/TiO_2$. This technique allowed us to monitor the dynamics of reaction product formation with high chemical sensitivity and in real ultrafast time scale.
The femtosecond resolution soft X-ray photoemission spectroscopy results are combined with theoretical calculations to provide crucial insight concerning reaction mechanisms and dynamics. Furthermore, the observation of subtle transient core level shifts provides information on interfacial charge transfer during the initial steps of the reaction immediately following the formation of the photogenerated charge carriers [1-3].

[1] Photoinduced Dynamics at the Water/TiO_2(101) Interface, Phys. Rev. Lett. 130 (2023) 108001.
[2] Ultrafast Real-Time Dynamics of CO Oxidation over an Oxide Photocatalyst, ACS
catalysis 10 (2020) 13650 – 13658.
[3] Dynamics of CO Photooxidation to CO_2 on Rutile (110), accepted in CommChem.

Melting, Bubblelike Expansion, and Explosion of Superheated Plasmonic Nanoparticles

Simon Dold
European XFEL

Matter under extreme conditions, especially at extreme temperatures and pressures, plays an important role in many fields. These range from astrophysics and geology over inertial fusion reactor studies to applied research on material processing by laser ablation. Due to the complex behaviour of matter under such conditions, the underlying interactions are not yet fully understood. In our study, we applied time-resolved soft X-ray diffraction at FLASH to study the dynamics of superheated silver nanoparticles in a laser pump – FEL probe experiment. The experiment reveals a broad range of different particle responses that can be traced back to the stability limits of a metastable superheated liquid.

Visualizing the Three-Dimensional Arrangement of Hydrogen Atoms in Organic Molecules by Coulomb Explosion Imaging

A. E. Green[1]

[1] *EaStCHEM School of Chemistry, University of Edinburgh, Edinburgh EH9 3FJ, U.K.*

E-mail: alice.e.green@ed.ac.uk

High-precision imaging of ultrafast structural dynamics of photoexcited molecules as they evolve on femtosecond timescales remains an elusive goal of modern chemical physics. Given the applications of photochemistry across many modern technologies, new tools to advance our fundamental mechanistic understanding may be crucial. One promising technique that has been driven forward recent years by developments in XFEL technology, particularly at the EuXFEL, is time-resolved Coulomb Explosion Imaging (CEI). In a CEI experiment, the target molecule is rapidly multiply ionized, prompting a prompt, violent fragmentation into several ions. By measuring the ions' relative momenta, the structure of the molecule prior to ionization can be inferred. If ionization is induced by an intense X-ray pulse, relatively large molecules can be rapidly and extensively fragmented, revealing detailed structural insights [1].

Here we demonstrate how X-ray induced CEI can be used to extract detailed three-dimensional structural information on a prototypical organic molecule: 2(5H)-thiophenone [2]. Importantly, we can visualize the arrangement of all atoms within the molecule, including the light hydrogens. The arrangement of hydrogen atoms is of great importance in photochemistry, but hydrogen atoms are effectively hidden from alternative ultrafast diffractive imaging techniques. Supported by *ab initio* molecular dynamics simulations, we suggest that tracking the three-dimensional arrangement of peripheral hydrogen atoms with X-ray CEI may disentangle complex nuclear motions at the heart of fundamental photochemical transformations, such as photoisomerizations [3,4].

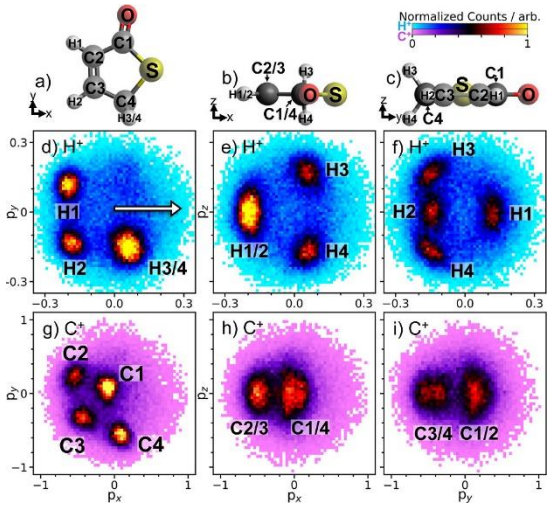

Fig.1: Example relative ion momentum images obtained following X-ray CEI of thiophenone – bearing close resemblance to the molecular structure.

References

[1] R. Boll *et al.* Nat. Phy. **18**, 423-428 (2022).
[2] A. E. Green *et al.* J. Am. Chem. Soc. **147**, 37133-37143 (2025).
[3] S. Pathak *et al.* Nat. Chem. **12**, 795-800 (2020).
[4] J. P. F. Nunes *et al.* J. Am. Chem. Soc. **146**, 4134-4143 (2024).

Electronic Molecular Movies with FELs: The Ultrafast Dynamics of 2-thiouracil

Fabiano Lever

Deutsches Elektronen-Synchrotron DESY, Hamburg, Germany

Light-induced ultrafast reactions play a fundamental role in the photophysics of DNA, as they can lead to the formation of lesions in the genetic code. Thionucleobases are sulfur-substituted nucleobases that show an increased rate of UV-induced lesion formation. In this talk, we investigate the photoinduced dynamics of 2-thiouracil (2-tUra) by combining time resolved XPS [1] and Coulomb explosion imaging (CEI) [2]. A UV pump excites 2-tUra into the S2 (ππ*) state and the subsequent dynamics are probed via both sulfur-localized 2p core excitation and CEI.

Time-resolved XPS traces image the excitation of the S1 (nπ*) state within ~100 fs and resolve a 200–250 fs oscillatory exchange among electronic states. Complementary CEI data directly visualizes the ultrafast symmetry reduction that enables the S2→S1 internal conversion: proton emission patterns report an out-of-plane deformation beginning within ~60 fs at the C2 site, followed by delayed motion of the sulfur atom, consistent with breaking planar Cs symmetry during passage through the conical intersection. Together, XPS and CEI correlate changes in electronic character with the geometric deplanarization of the molecular frame, providing a unified molecular-movie-level description of the coupled electronic and nuclear dynamics in 2-thiouracil.

1. Mayer, Lever et al. Nat Comm 13, 198 (2022)
2. Jahnke et al. Nat Comm 16, 2074 (2025)

Soft-X-ray ARPES from Static to Out-of-Equilibrium Electronic States

V. N. Strocov[1]

[1] *Swiss Light Source, Paul Scherrer Institute, 5232 Villigen-PSI, Switzerland*

E-mail: vladimir.strocov@psi.ch

Fundamental characteristics of solid-state systems such as electron dispersions, Fermi surfaces, and electron–boson coupling resolved in **k**-space, are essential for understanding their physical properties. ARPES provides direct access to this information. Compared with conventional VUV-ARPES, soft-X-ray ARPES offers three key advantages: a probing depth increased by a factor of 3–5, a proportionally sharper definition of the three-dimensional **k**, and element and chemical-state specific resonant photoexcitation. These properties make soft-X-ray ARPES ideally suited for studies of 3D bulk materials, buried interfaces/ heterostructures and impurity systems, including those forming functional blocks of electronic and quantum devices.

Numerous applications of static soft-X-ray ARPES to bulk materials, including topological systems, are illustrated with VSe_2 the van-der-Waals compound where 3D nesting of the Fermi surface forms 3D charge-density waves [1]. Applications to buried semiconductor interfaces are demonstrated by AlGaN/GaN high electron mobility transistor (HEMT) heterostructures, where we resolve the Fermi surface, band dispersions and Fourier composition of the interfacial quantum-well states [2]. An example of impurity systems is the Mn-doped GaAs, where resonant Mn *L*-edge photoexcitation identifies the ferromagnetic Mn impurity band and its hybridization with host GaAs [3].

Out-of-equilibrium soft-X-ray photoemission experiments are currently limited to tr-XPS at the SXP instrument of XFEL. Recent examples include the van der Waals material $TaSe_2$, where monitoring the Ta 4*f* core levels reveals laser-induced melting and re-formation of charge-density waves. Another case is the narrow-gap semiconductor InAs, in which laser-induced population of the conduction band competes with rapid diffusion of electrons into the bulk, producing a surface dipole layer (photo-Dember effect) that manifests itself in anomalous temporal evolution of the In 4*d* core levels at both negative and positive delays. Finally, I discuss routes to extend the SXP capabilities towards ARPES. These include operation in grazing-incidence geometry to increase photoelectron yield by a factor of a few tens, and an upgrade of the **k**-microscope with a repeller electrode to mitigate space-charge effects.

References

[1] V. N. Strocov *et al.*, Three-Dimensional Electron Realm in VSe_2 by Soft-X-Ray Photoelectron Spectroscopy: Origin of Charge-Density Waves, Phys. Rev. Lett. **109**, 086401 (2012)

[2] L. L. Lev *et al.*, **k**-space imaging of anisotropic two-dimensional electron gas in GaN-based high-electron-mobility transistor heterostructures, Nature Comm. **9**, 2653 (2018)

[3] M. Kobayashi *et al.*, Unveiling the impurity band induced ferromagnetism in the magnetic semiconductor (Ga,Mn)As, Phys. Rev. B **89** (2014) 205204

X-ray vision - revealing hidden structures with chemical imaging

Stephen Price

Finden Ltd./University of Sheffield (UK)

X-rays are a powerful tool for structural characterization, however conventional single point measurements do not always capture the full picture of chemical or structural heterogeneity that can be present in a sample. This is particularly the case when considering manufactured items and functional devices such as pharmaceutical tablets, batteries and chemical reactors, but can also be present in natural substances such as teeth. This talk will present an overview of recent research conducted using the chemical imaging technique of X-ray diffraction computed tomography (XRD-CT), and show how using this special "X-ray vision" reveals a deeper understanding of the chemical and physical structures within objects, that can be used to improve on their synthesis, manufacture and performance.

Shaping Glasses with X-Rays

G. Monaco
Dipartimento di Fisica ed Astronomia, Università di Padova, Padova, Italy

Illuminating an insulating or semiconducting glass using X-rays changes the properties of the glass, no matter what dose and dose-rates are used. The reason behind this is the complexity of the energy landscape of glasses, characterized by a huge number of different minima: during x-ray illumination the glass becomes an active system, powered by the absorbed energy, and explores this landscape. An x-ray illuminated glass becomes then the playground to study, under controlled conditions, phenomena which also appear in other contexts.
On the basis of x-ray photon correlation spectroscopy combined with nano-calorimetry experiments, I will discuss how x-ray irradiation can be used to prepare rejuvenated, high-enthalpy glasses [1,2]. In particular, while enthalpy increases with irradiation in a first stage, a sufficiently long irradiation results in a stationary state, independent of the initial state of the glass. The transition to this stationary state corresponds to the yielding transition [3].

[1] J. Baglioni et al., Rep. Prog. Phys. 87, 120503 (2024).
[2] J. Baglioni et al., Newton 2, 100338 (2026).
[3] A. Martinelli et al., Phys. Rev. X 13, 041031 (2023).

Quantum technologies meet functional materials: What X-rays can reveal

Martina Müller
Fachbereich Physik, Universität Konstanz

Quantum technologies and functional electronic materials share a common challenge: their performance is ultimately governed by electronic structure, defects, and interfaces on the atomic scale. Synchrotron-based X-ray spectroscopy provides a powerful and unifying toolbox to probe these properties with elemental, chemical, and depth sensitivity. In this talk, we demonstrate how hard X-ray photoelectron spectroscopy methods can reveal key microscopic mechanisms in materials relevant both for emerging quantum devices and for energy-efficient functional components.

For quantum technologies, the realization of stable and scalable qubits requires materials with precisely engineered electronic states and minimal sources of decoherence. We investigate the electronic structure of silicon and germanium-based qubits. By probing band structures, defect states, and interface electronic properties, hard X-ray momentum microscopy enables the identification of material (im)perfections that limit coherence times and device fidelity.

Beyond quantum materials, we also focus on ferroelectric oxides as a class of functional materials with high relevance for energy-efficient electronics. Hafnium oxide (HfO_2)–based thin films and their doped variants exhibit robust ferroelectricity at the nanoscale while remaining compatible with CMOS technology. This unique combination makes them promising candidates for non-volatile memories, ferroelectric field-effect transistors, novel logic elements, and high-energy-density capacitors. The stabilization of ferroelectric phases in HfO_2 depends sensitively on dopants and interfaces - parameters that can be accessed in detail using HAXPES.

Structural features of lignin based thermosets

Mats Johansson, Professor

Department of Fibre & Polymer Technology
Wallenberg Wood Science Center
KTH Royal Institute of Technology
SE-100 44 Stockholm, Sweden

Thermoset polymers are complex macromolecular structures where the macroscopic properties depend on several different structural features such as crosslink density, rigidity on a molecular level, and internal secondary bond interactions. Molecular rigidity is often induced by the incorporation of aromatic structures in the polymer network and these are often derived from the fossil oil based BTX-platform (benzene, toluene, xylene). The replacement of these BTX-based monomers with bio-based alternatives is desirable from a sustainability perspective and here is lignin one of the few alternatives available in large enough quantities. Lignin however present a significantly more complicated structure being a polydispese macromolecule with structural features not only depending on the lignin source but also how lignin has been retrieved from the original source. It is far from clear how these structural features affect the final properties of thermoset when being incorporated into a network structure.

The presentation will describe how a combination of several advanced chemical characterization techniques combined with different X-ray scattering studies can reveal improved understanding of the structure – property relationship of lignin based thermoset materials.

Catching Matter in the Act: Real-Time Observation of Phase Transformations at Conditions Approaching 1 Mbar and 5000 K

Emma Ehrenreich-Petersen

On behalf of all participants during four 2-year Long-Term Proposals at beamline P02.2, DESY.

The Extreme Conditions Beamline P02.2 at DESY specializes in X-ray diffraction (XRD) in diamond anvil cells (DACs), where pressures up to 6 megabar and temperatures up to 10000 K are accessible. Building on this capability, several Long Term Proposals (LTPs) led by Lawrence Livermore National Laboratory have significantly expanded the scientific scope of the beamline by combining X-ray phase contrast imaging (XPCI) with simultaneous XRD in the DAC, the first implementation of this kind at a synchrotron. We will discuss the development of these LTPs, focusing on how this combined approach has been used to quantify kinetic effects as a function of compression rate, to determine melting lines with high accuracy and precision, and how we have used XPCI to study viscosity at pressures approaching 1 Mbar. We will also discuss how the joint use of XPCI and XRD provides a hierarchical view of DAC samples, improving our understanding of their internal behavior and yielding new insights into kinetic processes and deep Earth relevant phenomena. And for the future? LTP number 5 will start this year focusing on further method and instrument development in preparation for the new Extreme Conditions Time Resolved XRD and Imaging Microscope (ExTReM) beamline at PETRA IV.

Poster List

Poster Session I / 27. 1. 26 / European XFEL / Schenefeld

Poster 1-101 and 336

Poster Session II / 28. 1. 26 / FLASH, External/Theory/Other, DESY

Poster 102 – 191, 337 and 338

Poster Session III / 29. 1. 26 / PETRA III, DESY

Poster 192 – 335

II Poster Session Topics

II.1 European XFEL

1. Developing a Pulse-Shaping Tool for DiPOLE100X at the EU-XFEL
   T. Aughey, E. Brambrink, J. Spear, A. Descamps, M. Streeter and E.E. McBride

2. AI Agent Support for Data Analysis
   T. Fuchs, L. Gelisio, S. Hauf and W. Maalej

3. Developments in Liquid Sample Delivery at the European XFEL
   E. Galtry, J. Valerio, K. Dörner, H. Han, E. Delmas, A. Wrona, A. Gierke, G. Pena, D. Choi, S. Kang and J. Schulz

4. Carbon contamination of EUV/X-ray optics
   A. Horynova and S. Schmidtchen

5. Crystallisation kinetics of liquid palladium
   Z. Kostera, P. Dziegielewski, R.Sobierajski and J. Antonowicz

6. Time, Spectral and Beam Focus Diagnostics in the SQS Instrument
   J. Montano, T. Baumann, R. Boll, S. Dold, A. de Fanis, M. Grunwald-Delitz, A. Igharas, A. Judt, S. Kudagama, T. Mazza, Y. Ovcharenko, D. Raiser, N. Rennhack, M. Robinson, M. Togawa, S. Usenko, S. Venkatesh and M. Meyer

7. Capturing ultrafast electron dynamics in batteries using XFELs
   M. Othman, A. Sarkar, F. Alves Lima, Y. Uemura, A. Bonucci, K. Haldrup, M. M. Nielsen, M. T. Wachter-Lehn, A. O. Dohn, M. Haubro, J. M. G. Lastra, I. E. Castelli, M. Dillenz, J. M. Castillo Robles, J.-M. Tarascon, O. Sel, A. Chaupatnaik, M. Deschamps, Z. R. Tan, H. B. Aguiar, M.-R. Amara, H. Yang, P. Siffalovic, R. Pandya and C. Milne

8. In-operando Interferometric Thickness Mapping of Liquid Flat-Jets with Sub-10 nm Resolution
   R. Ullah, S. Lucks, A. Przystawik, D. Diaman, M. Namboodiri, S. Skruszewicz and T. Laarmann

9. Timing-tool at the Femtosecond X-ray Experiments (FXE) instrument of the European XFEL: sub-100fs time resolution and new development
   H. Wang, H. Xu, Y. Jiang, J. Liu, P. Zaden, M. Knoll, P. Frankenberger, H. Yousef, M. Biednov, X. Huang, Y. Uemura and C. Milne

10. Generation of attosecond X-ray FEL pulses carrying orbital angular momentum
    C. Xu, J. Yan, G. Geloni, C. Lechner and H. Deng

11. High-power hard X-ray attosecond pulse generation at the European XFEL
    C. Xu, Y. Chen, W. Decking, M. Guetg, S. Liu, T. Long, W. Qin, U. Boesenberg, G. Geloni, N. Kuiala, A. Madsen, I. Inoue and J. Yan

12. Ultrafast Coherent Diffraction Imaging and Bragg CDI On Individual Gold Nanoparticles
    R. Buchin, R. Radloff, J. Leutloff, N. Muthreich, S. Grimm, I. Inoue, S. Skruszewicz, H. Zhang, S. Gieschen, H. Meyer, S. Dold, X. Liu, R. de Wijn, L. Worbs, F. Trost, Y. Kim, K. Kharitonov, E. Sobolev, S. Sahel-Schackis, S. Mous, S. Boutet, A. Aquila, J. Bielecki, C. Bostedt, F. Schulz, S. Kuschel and T. Gorkhover

13. Depletion-Induced Interactions Modulate Nanoscale Protein Diffusion in Polymeric Crowder Solutions
    M. Dargasz, N. D. Anthuparambil, S. Retzbach, A. Girelli, S. Timmermann, J. Möller, W. Jo, A. Leonau, A. M. Raza, M. Bin, J. Savelkouls, I. Andronis, F. Unger, F. Brausse, J. Hallmann, U. Boesenberg, J. Pudell, A. Rodrigues-Fernandezand, J. Wrigley, R. Shayduk, M. Youssef, A. Zozulya, A. Madsen, F. Lehmkühler, F. Perakis, F. Zhang, F. Schreiber, M. Paulus and C. Gutt

14. Investigation of Charge, Spin and Lattice Entanglement In Properties of $LaCoO_3$
    H. Firoozi

15. Measurement of neon photoemission delays and double-core-hole Auger-Meitner lifetime using Angular Streaking
L. Funke

16. XFEL anomalies in nuclear resonance scattering: From fundamental understanding to non-invasive precision probes
M. Gerharz, L. Yagüe Bosch, J. Evers and R. Röhlsberger for the ^{57}Fe EuXFEL collaboration

17. Iron at extreme condition at the EuXFEL: static and dynamic experiments
H. Ginestet, S. Merkel, community proposals EuXFEL 2740, 3063, 5700 and 6659

18. Temporal evolution of X-ray fluorescence of highly charged xenon ions under FEL irradiation
M.J. Grunwald-Delitz, T.M. Baumann, M. Meyer, J. Söderström and J.-E. Rubensson

19. Formation of high-spatial frequency LIPSS on metals probed by fs-time-resolved small-angle X-ray scattering
D. Kaczmarek, A. Rudenko, T.J. Albert, M. Weise, J. Antonowicz, F. Capotondi, R. Carley, D. Chopra, T. Derrien, P. Dzigielewski, L. Le Guyader, Z. Kostera O. Liubchenko, L. Mercadier, G. Mercurio, R. Minikayev, M. Mo, M. Pancaldi, E. Pedersoli, A. Scherz, R. Sobierajski, Y. Sun, M. Teichmann, A. Valerio, P. Zalden, J.-P. Colombier, J. Bonse and K. Sokolowski-Tinten

20. Insights into the structural and dynamic behaviour of biopolymers through collaborative measurements with SAXS and MHz-XPCS
A.M. Roda Lentz, M. Paulus, M. Dargasz, D.C. Florian Wieland and C. Gutt

21. Isolating the X-ray Thermal Diffuse Scattering signal from coated-copper targets under shock compression
D. J. Peake, P. G. Heighway, T. Stevens and J. S. Wark

22. Two-colour pump-probe measurements of transition rates in isochorically heated iron
C. Prestwood, T. Preston, U. Zastrau, M. Mishchenko, E. Bambrink, M. Nakatsutsumi, Z. Konôpková, M. Andrzejewski, R. S. Venkata, S. Göde, L. Randolph, S. Vinko, K. K. Alaa El-Din, H. Taylor, C. Crèpisson, J. P. Naedler, Q. ChongBing, D. Kraus, H. J. Lee, B. Nagler, N. Hartley, M. Šmid, H. Höppner, C. Baehtz, A. L. Garcia, J. P. Schwinkendorf, C. Palmer and O. Humphries

23. Time-resolved structural dynamics inphotoexcited molecular systems
M. Sekkal, Z. Nurekeyev, H. Hwang, S. Dutta, H. Wang, V. Markmann, B. Steinmann, D. Ronchetti, T. Baumann, R. Bauer, A. Eriksson, C. Bömer, M. Busi, T. Choi snd S.J. Goodner, F. Otte, R.D. Schaller, K. Haldrup, D.J. Gosztola, M. Kushniyarov, C. Bressler, K. Kubicek and A. Jacobi von Wangelin

24. Spectroscopy of ultrafast dynamics in trapped highly charged ions
M. Togawa, J. Crespo Lopez-Urrutia, T. Pfeifer, M. Meyer and T. Baumann

25. Femtosecond Three-Dimensional Imaging of Single-Protein with Hard X-ray Laser
P. L. Xavier, A.J. Morgan, J. Bielecki, R. Bean, C. Li, A.K. Samanta, W. Zhang, J. E, F. Koua, L. Gelisio, O. Turkot, E. Sobolev, M. Butola, O. Yefanov, S. Rafie-Zinedine, S. Dold, M. Meyer, M. Porro, F. Trost, C. Kim, T. Sato, L. Haas, J. Lübke, J. He, M. Memovich, K. Janson, S. Lenzen, E. Round, C. Schmidt, R. Alvarez, E.C. Yang, S. Wang, M. Miranda, H. Shen, A. Courbet, N.M. Ennist, E. Chia, R. Sha, M. Azubel, D.A. Bushnell, S. Boutet, S. Ovchinnikov, N. King, A. Barty, F. Maia, R. Kirian, A.V. Martin, T. Grant, N.D. Loh, S. Bajt, J. Küpper, R.D. Kornberg, D. Baker and H.N. Chapman

26. Femtosecond Holographic Single-Particle Diffractive Imaging of RNA-Polymerase with Atomic Cluster References using Hard X-ray Laser
P. L. Xavier, M. Azubel, D.A. Bushnell, A.J. Morgan, J. Bielecki, R. Bean, C. Li, A.K. Samanta, W. Zhang, J. E, F. Koua, L. Gelisio, O. Turkot, E. Sobolev, M. Butola, O. Yefanov, S. Rafie-Zinedine, S. Dold, M. Meyer, F. Trost, C. Kim, T. Sato, L. Haas, J. He, M. Memovich, K. Janson, S. Lenzen, E. Round, C. Schmidt, R. Alvarez, E.C. Yang, S. Wang, M. Miranda, H. Shen, A. Courbet, N.M. Ennist, E. Chia, R. Sha, S. Boutet, S. Ovchinnikov, N. King, A. Barty, F. Maia, R. Kirian, A.V. Martin, T. Grant, N.D. Loh, S. Bajt, J. Küpper, D. Baker, R.D. Kornberg and H.N. Chapman

27. Ultrafast Charge Transfer across Strongly-Correlated Oxide Interfaces
T.C. Asmara, R.J. Green, J. Schlappa, S. Parchenko, C.W. Galdino, Y. Wei, Z. Zhang, Y. Tseng, N. Gerasimova, G. Merzoni, B. Van Kuiken, M. Teichmann, Y.-P. Chang, L. Mercadier, D. Chopra, E. Paris, W. Zhang, T. Yu, G. Mercurio, R. Carley, M. Radovic, T. Schmitt and A. Scherz

28. Mix-and-Inject Sample Delivery Systems for Time-resolved Serial Crystallography on the SPB/SFX instrument
M. Vakili et al.

29. The Single Particles, Clusters, and Biomolecules & Serial Femtosecond Crystallography (SPB/SFX) Instrument - Detector Systems
M. Vakili et al.

30. Status of the Long Term Proposal: Dynamics of nanoscale phenomena in solids and liquids studied with X-ray Transient Gratings at European XFEL
A. Cannizzo, M. Chergui, J.R. Rouxel, C. Masciovecchio, F. Bencivenga, D. Fainozzi, A. Madsen, C. Milne, R. Cucini, C. David, J. Vila-Comamala, T. Mamyrbayev, U. Staub, S. Bonetti, W. Błachucki, A. Maznev, K.A. Nelson, J. Szlachetko, W. Gawelda, T. Feurer, D.A. Reis, C. Serrat, E. Ferrari, M. Beye, R. Torre, M. Biednov, X. Huang, P. Frankenberger, S. Heder, F.A. Lima, F. Ardana-Lamas, M. Scholz, P. Zalden, H. Xu, M.R. Dhanalakshmi-Veeraraj, R. Mincigrucci, M. Brioschi, P. Carrara, G. Rossi, N.N. Khatu, R. Engel, E. Paltanin, M. Deb, N. Berndt, M. Bargheer, A. Gessini, M. Knoll, D. Ronchetti, L. Banares, N. Rohringer, A. Benediktovitch, C. Soncini, J.-E. Pudell, P.R. Miedaner, R. Rysov, S. Marotzke, S. Jackson, J. Ghosh, H. Li, L. Zhang, A. Schmidt, A. Udai, M. Savoini, D. Zhu and C. Svetina

31. Status and upgrades of the Split and Delay Line Unit at MID Instrument
R. Rysov, B. Friedrich, J. Hallmann, J. Möller, W. Jo, T. Noll, W. Lu, G. Ansaldi, S. Eisebitt and A. Madsen

32. FATRA, Fast Train Review Application
P. Szeles, P. Vagovič, J.C.P. Koliyadu, D. Moško, I. Draci and J. Uličný

33. Real-time visualization of asymmetric ligand binding and structural dynamics in human redox flavoenzyme NQO1
I. Quereda-Moraleda, M. Rivero, V. Correa, D. Doppler, M. Usón, A. Grieco, S. Boneta, M. Sonker, D. Koh, A. Manna, A. Ansari, R. Alvarez, K. Karpos, H. Le, S. Mahmud, R. Letrun, K. Dörner, J. C. P. Koliyadu, R. de Wijn, J. Bielecki, H. Han, C. Kim, F. H. M. Koua, A. Round, A. Sarma, T. Sato, C. Schmidt, M. Vakili, D. Zabelskii, R. Bean, J. Schulz, R. A. Kirian, S. Botha, A. L. Pey, A. Ros, M. Medina and J. M. Martin-Garcia

34. Using surface roughness to probe relativistic laser plasma interactions
S.V. Rahul, M. Banjafar, L. Randolph, T. Preston, N. Samadi, M. Makita, T. Kluge, L. Huang, J.P. Schwinkendorf, Ö.Öztürk, D. Ksenzov, T. Yabuuchi, K. Miyanishi, M. Nishiuchi, M. Ota, C. David, C. Gutt and M. Nakatsutsumi

35. Single-shot X-ray imaging of two-dimensional strain fields in colloidal crystals
J. Diao, J. Fan, I. Robinson and H. Jiang

36. Angular streaking reconstruction
D.E. Ferreira de Lima, P. Schmidt, I. Bermudez-Macias, T. Berberich, J. Ribbing, F. Bishara, T.M. Baumann, R. Boll, A. De Fanis, T. Mazza, D. Raiser, M.S. Robinson, S. Usenko, S. Serkez, A. Trebushinin, M. Guetg, G. Perosa, G. Geloni, M. Meyer and L. Gelisio

37. UK XFEL Project: Science and Technology Case for a Next Generation XFEL
J. Marangos on behalf of UK XFEL Project Team

38. Automating analysis workflows
J. Wrigley

39. Handling detectors geometry and bad pixels at European XFEL
O. Turkot

40. Automating Alignment Workflows at European XFEL
S. Birnsteinova, R. Bean, J. Bielecki, F. Dall'Antonia, D. Doblas-Jiménez, D. Enoque Ferreira de Lima, A. Garcia-Tabares, L. Gelisio, S. Hauf, I. Karpics, J. Koliyadu, R. Letrun, T. Michelat, J. Möller, E. Sobolev, F. Sohn, O. Turkot, R. de Wijn and P. Zalden

41. Exploring Electron Dynamics in Chiral Molecules with Free-Electron Lasers
M. Ilchen on behalf of a large collaboration

42. A novel approach to the molecular dynamics analysis via X-ray diffraction
A.M. Jumbo Nogales, Z. Shen and K. Ayyer

43. Online Analysis of MHz XPCS with AGIPD at MID-EuXFEL
M.B. Jakobsen, J. Möller, J. Wrigley, A. Leonau, A. Zozulya, J. Hallmann, T. Guest, P. Schmidt, D. Hammer, A. Madsen and L. Gelisio

44. Overview of the SQS scientific instrument at European XFEL
S. Usenko, A. Alangattuthodi, T. Baumann, R. Boll, A. De Fanis, S. Dold, M. Grunwald-Delitz, A. Igharas, A. Judt, S. Kudagama, S. Makam, T. Mazza, J. Montano, N. Morozov, Y. Ovcharenko, D. Raiser, N. Rennhack, M. Robinson, S. Sasikumar, K. Shaw, M. Togawa and M. Meyer

45. MHz X-ray imaging capabilities at the European XFEL
J.C.P. Koliyadu, D. Mosko, P. Szelses, C. Kim, P. Kaul, P. Fischer, J. Uličný, R. Bean, A. Meents, T. Sato and P. Vagovič

46. Detectors at the SCS Instrument, current status and future developments
L. Le Guyader, J. Schlappa, N. Gerasimova, G. Mercurio, J.-T. Delitz, M. Ramilli, D. Lomidze, M. Turcato, M. Porro and A. Scherz

47. Advanced Structural and Physicochemical Characterization of CuO Nanoribbons for Biosensing Applications
N. Ghodrati, G. Feraco, D.D. Jimenez, H. Han, R. Schubert, V. Bazhenov, C. Deiter, A. Sarkar and M. Izquierdo

48. Modeling processes leading to cascaded ion emissions from copper plasmas produced by an X-ray free-electron laser
T. Burian, J. Krása, M. Stransky, Z. Jurek, L. Juha and collaborators

49. Probing the Formation of Laser-Induced Periodic Surface Structures on Metals by Ultrafast Time-Resolved Grazing Incidence X-ray Scattering
L. Randolph, Ö. Öztürk, D. Kaczmarek, O. Liubchenko, T. J. Albert, M. Andrzejewski, J. Antonowicz, J. P. Colombier, S. Goede, H. Hoeppner, L. Huang, G. Jakob, M. Kläui, T. Kluge, D. Ksenzov, A. Leonau, M. Makita, M. Mishchenko, M. Mo, T. R. Preston, S. V. Rahul, B. Rethfeld, C. Rödel, A. Rudenko, M. Sahre, J.-P. Schwinkendorf, R. Sobierajski, Y. Sun, F. Unger, S. T. Weber, M. Weise, P. Zalden, C. Gutt, K. Sokolowski-Tinten, J. Bonse and M. Nakatsutsumi

50. Contributions of European XFEL to DAPHNE4NFDI
F. Dall'Antonia, C. Carinan and L. Gelisio

51. Burst-Mode CoRDIA – An Option for a Second-Generation Detector for the European XFEL
U. Trunk, A. Marras, A. Klujev, S. Lange, T. Laurus, D. Pennicard, C.B. Wunderer, H. Krueger and H. Graafsma

52. EBPFCat - an open source EtherCAT implementation for experimental control
M. Teichmann

53. FEL studies of Complex Metal Nanoparticles and their Structural Dynamics
S. Sasikumar, P. Piseri, S. Dold, Y. Ovcharenko, S. Usenko, D. Raiser, M. Robinson, C. Piazzoni, C. Callegari, M. Meyer and T. Mazza

Milexia

Making access to technology easier

Milexia ist ein **paneuropäischer Added-Value-Distributor** für **Hightech-Komponenten und Systeme** für eine Vielzahl von Technologien. Speziell im Bereich **High-Power RF & Microwave bieten** wir Komponenten wie

- **Zirkulatoren**,
- **flexible** und **feste Wellenleiter**,
- **Wasserlasten**
- und viele andere **aktive** und **passive Mikrowellenkomponenten**

von namhaften Herstellern wie **Microwave Techniques, Stellant, Narda-Miteq, Coaxicom** und weiteren Partnern an.

GET IN TOUCH TO LEARN MORE!

KONTAKTIEREN SIE UNS UND FINDEN SIE DIE PERFEKTE LÖSUNG!

+ 49 (0) 7131 7810-0
de-sales@milexia.com
www-milexia.com/de

MILEXIA®
MAKING ACCESS TO TECHNOLOGY EASIER

CRYSDIAM

Single crystal CVD diamond for Scientific instruments

Ultra Thin 10 Micron

Ultra Size 60 x 60 mm

Optical grade

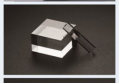

Size	Single crystalline < ϕ 50mm
Thickness	Single crystalline 0.01mm-3mm
Roughness (both sides)	<10nm (in 1mm²) * 2nm as request
Thermal conductivity	> 1900W/mK
Transmission rate (thickness 1mm)	1064nm >68% , 8-25m >70%
Refractive rate	104nm 2.392 , 600nm 2.415

Electronic grade / Quantum grade

Size	typical 5x5mm, 4x4mm
Thickness	0.05-0.5mm
Roughness (both sides)	<10nm (in 1mm²)
Thermal conductivity	> 2000W/mK
Nitrogen concentration	< 20ppb
Lattice	100, 110, 111
Banod gap width(ev)	5.47
Resistivity (Ω.cm)	>1010
Dielectric constant	5.5

info@andrews-instruments.de
Tel: 0049 40 2488 3840

andrews instruments GmbH
www.andrews-instruments.de

54. MHz-XPCS use case in the framework of the DAPHNE4NFDI project
A. Leonau, A. Tosson, N.D. Anthuparambil, M. Dargasz, F. Unger, A. Raza, Ö. Öztürk, R.P. Gautam, J. Wrigley, M. Teodoro, C. Carinan, R. Rosca, F. Dall'Antonia, J. Möller, A. Madsen, L. Gelisio and C. Gutt

55. Neural networks for 2-color FEL diffraction image separation
N. Morozov, D.E. Ferreira de Lima, D. Vetrov and Y. Ovcharenko

56. Support for new protein crystallography users at the European XFEL
P. Smyth, K. Dörner, I. Arkhipushkin, L. Babazadeh, V. Bazhenov, C. Deiter, E. Delmas, E. Galtry, A. Gierke, H. Han, M. Kloos, J. Moore, R. Schubert, C. Schmidt, J. Tolkiehn, J. Valerio, A. Wrona and J. Schulz

57. Ultrafast decoupling of polarization and strain in ferroelectric BaTiO3
G. Mercurio, L.P. Hoang, D. Pesquera, G.N. Hinsley, R. Carley, L. Mercadier, M. Teichmann, E.M. Unterleutner, D. Knez, M. Dienstleder, S. Ganguly, T.C. Asmara, G. Merzoni, S. Parchenko, J. Schlappa, Z. Yin, J.M. Caceido Roque, J. Santiso, I. Spasojevic, C. Carinan, T.-L. Lee, K. Rossnagel, J. Zegenhagen, G. Catalan, I. Vartaniants and A. Scherz

58. High-field Terahertz and mid-IR Light Sources for Time-resolved Studies at European XFEL
I. Radu, R. Ivanov, B. Monoszlai, D. Rompotis, J. Meier, R. Secareanu, M. Emons, D. Kane, D. Sequeira, A. Kartal, S. Venkatesan, J. Wang, S. Hoseinkhani, U. Wegner and M. Lederer

59. Experimental-technique-oriented data analysis documentation
I. Bermudez on behalf of the data analysis team

60. We watch a ring molecule open and close using Coulomb explosion imaging
B. Richard, M. Robinson, J. Merrick, F. Allum, D. Heathcote, T. Janke, J. Rigden, S. Usenko, T. Walmsley, E. Anderson, Y. Biddick, A. Edmonds, N. Mitchell, R. Boll, A. Butler, R. Ingle, F. Lever, H. Lindenblatt, T. Mazza, D. Meyer, P. Nunes, D. Raiser, C. Rankine, P. Schmidt, B. Senfftleben, J. Thompson, L. Inhester, M. Gühr, A. Kirrander, R. Santra, C. Vallance, M. Meyer and P. Robertson

61. Towards accurate simulation of X-ray-induced Coulomb explosions
B. Richard, Z. Jurek, R. Santra and L. Inhester

62. DAMNIT-web: Automated experiment overviews, now in the browser
C. Carinan and R. Rosca on behalf of the DAMNIT team of the Data Analysis group

63. Data management infrastructure for European XFEL.
J. Malka, C. Voss, D. Boukhelef, F. Schluenzen, G. Previtali, J. Szuba, J. Hannappel, K. Hoyos, K. Ohrenberg, K. Schwarz, K. Filippakopoulos, K. Wrona, L.M aia, M. Sahakyan, M. Gasthuber, M. Karimi, P. Suchowski, R. Lueken, S. Dietrich, S. Aplin, S. Sternberger, T. Mkrtchyan, T. Piszczek and Y. Kemp

64. Implementation of a new European XFEL scientific data policy.
J. Malka, E. Sobolev, F. Dall'Antonia, G. Winterhoff, I. Bermudez Macias, J. Szuba, K. Wrona, L. Gelisio, L. Maia, O. Turkot, P. Schmidt, S. Aplin and W-T. Tsai

65. Proposal Lifecycle Services at EuXFEL with myMdC
L. Maia, S. Aplin, D. Boukhelef, F. Dall'Antonia, I. Derevianko, L. Gelisio, D. Goeries, S. Hauf, N. Liss, J. Malka, M. Manetti, G. Previtali, P. Schmidt, V. Singh, J. Szuba, W. T. Tsai, B. Vanganuru and K. Wrona

66. MyLog: A modern, integrated logbook for scientific collaboration at European XFEL
L. Maia, A. Anakkappalla, S. Aplin, D. Boukhelef, F. Dall'Antonia, I. Derevianko, L. Gelisio, D. Goeries, S. Hauf, J. Malka, M. Manetti, T. Michelat, G. Previtali, P. Schmidt, V. Singh, J. Szuba, W.-T. Tsai, B. Vanganuru and K. Wrona

67. Fluctuation X-ray Scattering: from theory to experimental structure determination of the PR772 virus
T.B. Berberich and R.P. Kurta

68. CdZnTe Sensor Characterization at European XFEL using JUNGFRAU - Beyond the Standard Flux
S. Palutke, D. Greiffenberg, J. F. Mulvey, K. A. Paton, M. Ramilli, B. Schmitt, M. Sikorski and M. Turcato

69. Laser-induced alignment of macromolecules and nanoparticles
L. V. Haas, X. Cheng, M. Amin, J.-M. Hartmann, C. Heinze, A. Samanta and J. Kuepper

70. Online Analysis Integration
D. Hammer

71. Highspeed imaging of laserinduced cavitation in porcine eyes
D. Miesner, J. Rossello and T. Salditt

72. The Pump-Probe Laser at the Small Quantum Systems (SQS) Instrument at European XFEL.
A. Alangattuthodi, P. Grychtol, A. Igharas, J. Montaño, T. Mullins, D. Raiser, N. Rennhack, D. Rivas, M.S Robinson and M. Meyer

73. Does Rotation Matter? Mapping Charge Transfer In Dissociating Molecules
B. Senfftleben, F. Allum, L. Banares, M. Burt, I. Casasús, T. Chou, M. E. Corrales, A. de Fanis, R. de Nalda, A. Duley, B. Erk, A. Green, H. Lam, X. Li, B. Maingot, T. Mullins, Y. Ovcharenko, S. Marggi Poullain, D. Raiser, P. Recio, D. Rolles, A. Rouzee, A. Rudenko, K. Shaw, S. Usenko, E. Warne, T. Walmsley, E. Wang, T. Witting, M. Meyer and R. Boll

74. Quantum-state-resolved X-ray multiphoton ionization dynamics
S.-K. Son, T.M. Baumann, S. Cardoch, N. Tîmneanu, M. Meyer, R. Santra and J.-E. Rubensson

75. Status of FAST-XPD: Photon Database for the European XFEL
M. Manetti, L. Samoylova, H. Sinn, J. Szuba, K. Wrona, M. Yurkov and I. Zagorodnov

76. Sample Characterization at the User Labs of the European XFEL
C. Deiter, I. Arkhipushkin, L. Babazadeh, V. Bazhenov, E. Delmas, K. Dörner, E. Galtry, H. Han, M. Kloos, J. Moore, C. Schmidt, R. Schubert, P. Smyth, J. Tolkiehn, J. Valerio and A. Wrona

77. Lipoprotein Diffusion in Dense Yolk Plasma is Governed by Softness, Hydrodynamics, and Caging: Insights from MHz-XPCS
N. Das Anthuparambil, M. Dargasz, S. Timmermann, A. Girelli, S. Retzbach, J. Möller, W. Jo, A.M. Raza, A. Leonau, J. Wrigley, F. Unger, M. Bin, P.P. Rajaiah, I. Andronis, W. Chèvremont, J. Hallmann, A. Rodriguez-Fernandez, J.-E. Pudell, F. Brausse, U. Boesenberg, M. Youssef, R. Shayduk, R. Rysov, A. Madsen, F. Lehmkühler, M. Paulus, F. Zhang, F. Perakis, F. Schreiber and C. Gutt

78. European XFEL User Laboratories
H. Han, I. Arkhipushkin, L. Babazadeh, V. Bazhenov, C. Deiter, E. Delmas, K. Dörner, E. Galtry, A. Gierke, M. Kloos, J. Moore, C. Schmidt, R. Schubert, P. Smyth, J. Tolkiehn, J. Valerio, A. Wrona and J. Schulz

79. Standard Sample Preparation for Serial Femtosecond Crystallography
C. Schmidt, K. Lorenzen, J. Schulz and H. Han

80. Single-particle incoherent diffractive imaging and amplified spontaneous emission in copper nanocubes
T. Wollweber, S. Dutta, Z. Shen, J. Bielecki, C. Caleman, S. Cardoch, A. Estillore, L. Haas, S. Karl, F. Koua, A. Mall, P. Mazumder, D. Melo, M. Prasciolu, O. Rambadey, A. Samanta, A. Sarma, T. Sato, E. Sobolev, F. Trost, S. Bajt, R. Bean, J. Küpper, N. Timneanu, R. Röhlsberger, J. von Zanthier, F. Schulz, H. Chapman and K. Ayyer

81. Borrowing high-energy physics algorithms for serial crystallography: detector alignment with Millepede-II
T.A. White

82. Characterization of focused time-delayed two-color XFEL beams by ablation imprints
Š. Jelínek, M. Šmíd, T. Burian, V. Vozda, L. Vyšín, V. Hájková, A. Horynová, L. Juha, D. Váňa, A. Laso Garcia, R. Sripati, O. Humphries, E. Brambrink, K. Appel, H. Höppner, M. Nakatsutsumi, M. Andrzejewski, D. Bespalov, A. Pelka, M. Kopecký, N. Medvedev, U. Zastrau and J. Chalupský

83. New cryogenic sample environments at the MID instrument
J. D. Moore, J. Schulz, J-E. Pudell and A. Madsen

84. An online analysis pipeline for MHz XPCS at EuXFEL
Mads B. Jakobsen, J. Möller, J. Wrigley, A. Leonau, W. Jo, A. Zozulya, J. Hallmann, T. Guest, P. Schmidt, D. Hammer, A. Madsen and and L. Gelisio

85. Segmented droplet injection for static and time-resolved serial crystallography
A. Ros et al.

86. Simulation User Interfaces - Concept and Design
R. Rosca and J. E

87. X-PULSE for Imaging of Foam Wetting at Cryogenic Temperatures for Inertial Fusion Energy Applications
R.L. Sandberg, A. Gleason, W. Sweet, J. Kline, S. Glenzer and C. Menoni

88. Magnetohydrodynamics Under Extreme Currents: Pulsed Power Experiments at Synchrotrons and XFELs
J. Strucka

89. Control and Data Acquisition Software at the European XFEL
EuXFEL Control Software Group

90. Karabo interfaces to other control systems
EuXFEL Control Software Group

91. The Chem endstation at the SCS Instrument: A versatile platform for ultrafast soft X-ray spectroscopy with liquid samples
B. Van Kuiken, Y.-P. Chang, L. Adriano, L. Le Guyader and A. Scherz

92. Investigating Driven Dynamics in Protein Solutions: First Insights from Optical Pump–XPCS Probe Experiments at MID
F. Unger, N. D. Anthuparambil, A. Leonau, J. Hallmann, J. Moeller, M. B. Jakobsen, M. Dargasz, R. P. Gautam, A. M. Raza, M. Puritscher, S. Retzbach, A. Zozulya, R. Shayduk, F. Zhang, F. Lehmkuehler, M. Paulus, A. Madsen, F. Schreiber and C. Gutt

93. Towards a unified analysis framework for reaction microscopy data analysis at European XFEL and FLASH.
Data Analysis, SQS instrument at European XFEL, Data Analysis and FL26 beamline at FLASH

94. AI Copilot For FEL Experiments
M. Ajami, S. Hauf, F. Bishara and P.A. Murena

95. Structure and polydispersity of aerosolized lipid vesicles by femtosecond X-ray FEL pulses
C. Neuhaus, M. Stammer, J. Alfken, M. Osterhoff, K. Komorowski, J. Bielecki, S. Rafie-Zinedine, R. de Wijn, R. Letrun, J. E, R. Bean and T. Salditt

96. Exploring Light-Induced Metastable Magnetic States in TbCo Using Circularly Polarized X-rays at the SCS Instrument
S. Parchenko, L. Le Guyader, N. Gerasimova, J. Schlappa, M. Teichmann, B. Van Kuiken, P. Hoang, D. Chopra, A. Å. Larsson, V. Kapaklis and A. Scherz

97. New AGIPD Detectors and Developments for the European XFEL
S. Fridman, H. Graafsma, H. Hirsemann, A. Klyuev, S. Lange, T. Laurus, D. Magalhaes, A. Marras, S. Schneider, O. Shefer-Shalev, T. Stoye and U. Trunk

98. Italy-Germany bilateral scientific cooperation at the European XFEL facility: current status and perspectives
R. Bean, M. Izquierdo, P. Luches, T. Mazza, C. Milne, P. Piseri and F. Stellato

99. Smart Data Labeling for Large Imbalanced Datasets
A. Majid, D. Ferreira de Lima and L. Gelisio

100. Serial femtosecond crystallography on protein nanocrystals delivered by aerosol injection system
Y. Kim, R. de Wijn, F.H.M.Koua, S.Kantamneni, J.E, E. Sobolev, D. Melo, O. Turkot, R. Schubert, A. Wrona, M. Kloos, L. Worbs, C. Wei, Q. Xie, M. Sikorski, A. Round, J. Koliyadu, R. Letrun, H. Han, J. Schulz, T. Sato, A. P. Mancuso, J. Bielecki, R. Bean and C. Kim

101. X-ray - optical pulse arrival monitor based on spintronic THz emitters
R. Carley, L. Mercadier, L. Le Guyader, T. C. Asmara, C. Broers, Y.-P. Chang, J. T. Delitz, M. Teichmann, N. Gerasimova, N. Ghodrati, L. P. Hoang, R. Ivanov, B. van Kuiken, J. Liu, G. Mercurio, G. Merzoni, S. Parchenko, I. Radu, A. Reich, J. Schlappa, T. Kampfrath, T. Seifert, H. Jaffres, N. Stojanovic, M. Gensch and A. Scherz

II.2 FLASH

102. Towards Time-Resolved XPS of 2-Thiouracil treated Au Nanospheres
J. Schwarz, D. Mayer, F. Lever, B. Bhattacharyya, L. Cordsmeier, S. Eckert, N. Jahn, S. Sinha, E. Titov, A. Taubert, P. Saalfrank, A. Föhlisch and M. Gühr

103. Concept design of transient grating instrument at Shenzhen FEL
Y. Zhong, X. Yang, J. Gao and Q. Yan

104. Imaging molecular fragmentation using Timepix detectors
H. Bromberger, O. Grabbert, A. Samartsev, C. Uden, S. Trippel, P. Stelldinger and J. Küpper

105. H. Bromberger and A. Sokol
Laser Performance Optimization Toolkit (LPOT)

106. Endstation for time-resolved X-ray photoemission spectroscopy at FELs
L. Wenthaus, D. Kutnyakhov, M. Heber, S. Palutke, H. Meyer, S. Gieschen and M. Martins

107. Data analysis at FLASH: The fab package
F. Lever and C. Passow

108. Development of 2nd generation of PERCVIAL Sensor and System for upgraded soft X-ray imaging
M. Hajheidari, C.B. Wunderer, A. Marras, M. Dahlgruen, J. Gebert, J. Correa, T. Hirono, F. Krivan, F. Scholz, J. Seltman, S. Lange, Th. Wendt, S.Y. Rah, I. Shevyakov, V. Vardanyan, M. Hoesch, K. Bagschik, N. Guerrini, B. Marsh, I. Sedgwick, G. Cautero, D. Giuressi, R.H. Menk, L. Stebel, A. Greer, T. Nicholls, W. Nichols, M. Nakhostin, H.J. Hyun, K.S. Kim, S.H. Kim, S.Y. Park, F.J. Iguaz, P. Baumgaertel and H. Graafsma

109. Non-linear autocorrelation measurement of an excessive reversed tapered undulator FEL in Ar gas
M. Dreimann, E. Schneidmiller, F. Lever, T. Reiker, V. Kärcher, D. Eckermann, R. Quenter, M. von Piechowski, P. G. Shine, D. Meyer, S. Roling, S. Toleikis, E. Plönjes, R. Treusch, M. Gühr and H. Zacharias

110. Ultrafast Charge Transfer Dynamics in a Plasmonic Photocatalyst Studied by Femtosecond Time-Resolved X-ray Photoelectron Spectroscopy
Z. Donnellan, K. Fung Lai, S. Perera, L. Hoffmann, M. Stapf, D. Potorochin, C. Perez, D. Glenna, Y. Joseph, L. Wenthaus, D. Kutnyakhov, N. Wind, S. Dziarzhytski, F. Pressacco, D. Neumark, W. Eberhardt, S. Molodtsov, F. Roth, J. Qian and O. Gessner

111. The FLASH1 THz Beamline After FLASH2020+ upgrade
S. Gang, M. Temme, E. Plönjes and R. Pan

112. Virtual Pulse Reconstruction Diagnostic for Single-Shot Measurement of Free Electron Laser Radiation Power
T. Korten, V. Rybnikov, P. Steinbach, M. Vogt, J. Roensch-Schulenburg and N. Mirian

113. URSA-PQ: A Mobile and Flexible Pump-Probe Instrument for Gas Phase Samples at FLASH
D. Mayer, F. Lever, X. Wang and M. Guehr

114. PESdata: Cross-Facility Open-Source Software for Multidimensional Photoemission Spectroscopy Data Analysis
D. Potorochin, M. Stapf, Z. Donnellan, L. Wenthaus, D. Kutnyakhov, O. Molodtsova, V. Aristov, S. Molodtsov, O. Gessner and F. Roth

115. Methods and Hurdles of live shot based polarization diagnostics at a free electron laser
M. Mogilowski

116. DRUMSOX Momentum Microscope coming to LCLS-II
J. Dilling, M. Scholz, L. Bruckmeier, M. Heber, J. Sobota, D. Liu, D. Puntel, P. Majchrzak, D. Kutnyakhov, N. Wind, L.Wenthaus, J. Koralek, Z.-X. Shen and K. Rossnagel

117. Quantum materials in action: Electronic, structural, and device innovations
L. Bruckmeier, M. Scholz, J. Dilling, C. Sharma, J. Buck, M. Heber, D. Kutnyakhov, N. Wind, L. Wenthaus, R. Blick and K. Rossnagel

118. Investigating Photoinduced Dynamics of a 1,4-Azaborine with Time-Resolved X-ray Spectroscopy at FLASH
K. Theil, M. Hess, C. Schouder, D. Mayer, F. Lever, X. Wang, R. Pan, U. Frühling, C. Papadopoulou, X. Miao, H. Braunschweig, M. Gühr, R. Mitric and I. Fischer

119. Investigating Photoinduced Dynamics of 4a,8a-Azaboranaphthaline with Time-Resolved X-ray-Spectroscopy at FLASH
D. Friedrich, K. Theil, S. Lutz, D. Schaffner, D. Mayer, F. Lever, X. Wang, M. A. Silva Toledo, F. Allum, M. Kuhlmann, M. Bühler, H.Helten, M.Gühr, M.I.S. Röhr and I. Fischer

120. FL28 - Angular Streaking for Temporal Photon Diagnostics
L. Wülfing

121. Unique Science Opportunities at the upgraded FLASH Facility
M. Gühr and R.Treusch for the FLASH Team

122. Unravelling proton transfer and fragmentation pathways in the water dimer cation in energy and time
I. S. Vinklárek, S. Trippel, M. Belina, L. Blum, H. Bromberger, P. Slavíček and J. Küpper

123. Data Pipeline and Analysis Workflow at FLASH
C. Passow and F. Lever

124. On the way to automatized focus adjustment at FLASH
B. Keitel, G. Brenner, S. Dziarzhytski, E. Plönjes, B. Schäfer, M. Lübbecke, K. Mann, J. Schmidt and G. Plonka

125. Wavelength, polarization and pulse duration diagnostics using photoelectron spectroscopy.
M. Braune, K. Tiedtke and M. Ilchen

126. FL28: A new diagnostic beamline for ultra-short XUV FEL pulses at FLASH
M. Walther, M. Ilchen, L. Wülfing, W. Helml, M. Braune, S. Düsterer and K. Tiedtke

127. FEL and HHG-based time-of-flight momentum microscopy: 3 time-resolved photoemission modalities in 1 experiment
D. Kutnyakhov, N. Wind, M. Heber, F. Pressacco, L. Wenthaus, H. Meyer, S. Gieschen and K. Rossnagel

II.3 Other topics, external facilities and theory

128. The European HyMetBat EPM project - Hybrid metrology for sustainable and low-carbon footprint battery materials
B. Beckhoff, on behalf of the HyMetBat consortium

129. An update of progress on the design of the diffraction line for the relativistic ultrafast electron diffraction and imaging facility at Daresbury Laboratory
J. Ouyang, B.R. Hounsell, A.R. Bainbridge, L.S. Cowie, J. Crone, M.J. Ellis, A. Farricker, A.J. Gilfellon, C. Hill, N.Y. Joshi, G. Marshall, J.W. McKenzie, B.L. Militsyn, T.C.Q. Noakes, T.H. Pacey, S.S. Percival, L.R. Reid, M.D. Roper, Y.M. Saveliev, E. Snedden, C. Tollervey, A.J. Vick, F. Yaman and Y. Murooka

130. CrSBr, a new photonic material: doping and magnetic control
B. Smette

131. Multimodal imaging with light microscopes and scanning small angle X-ray scattering
B. Yu, M. Sinha, R. Mendes Da Silva, U. Rölleke, M. Burghammer and S. Köster

132. Single-shot X-ray imaging of two-dimensional strain fields in colloidal crystals
J. Diao, J. Fan, I. Robinson and H. Jiang

133. FemtoMAX - a short pulse facility beamline at MAX IV
D. Kroon, J. C Ekström, B. Ahn, A. Jurgilaitis and J. Larsson

134. Microstructural insights into medium-entropy alloys
J. Kubaško, M. Matvija, K. Nigutová, L. Oroszová, Z. Molčanová, B. Ballóková, R. Džunda and K. Saksl

135. Pressure-induced tetrahedral-hexahedral-octahedral transition of GeO2 glass at high pressure
X. Hong

136. Fluorescence labeling of (Bio-)Nanoparticles for Optical Scattering Microscopy
S. Lenzen, K. Janson, L. Haas, J. He, S.K. Peravali, A. Estillore, M. Memovich, A.K. Samanta and J. Küpper

137. Impact of Attosecond X-ray Pulses on Electronic Damage Suppression in X-ray Diffraction
V. Lipp, I. Inoue and B. Ziaja

138. Spray high-efficiency organic solar cells
X. Jiang, K. An, N.Li and S.V. Roth

139. Mapping non-equilibrium reaction pathways via physio-chemical coupling at the pulsed irradiated solid-liquid interface
M. Sadegh Shakeri and Z. Swiatkowska-Warkocka

140. In Situ GIWAXS Analysis of Electric-Field-Induced Lattice Strain in Halide Perovskites Influenced by HTL Interfaces
S. Seo, S. Jeon and H. Kim

141. Single-Particle Imaging Using <100 Diffraction Patterns Assisted by Real-Space Constraints
Z. Shen and K. Ayyer

142. Novel High-Entropy Materials for Energy Storage
M. Hodorová, A. Fedoročkov'a, D. Csík, K. Gáborová, R. Džunda, G. Sučík, D. Ivánová, F. Kromka and K. Saksl

143. LONGITUDINAL PHASE SPACE RECONSTRUCTION IN THE KEK INJECTOR LINAC
A. Aguirre, I. Agapov, N. Iida and T.Mori

144. Near-Field Holotomography Reconstruction Using Implicit Neural Representations
J.P. Grün, S. Eberle, S. Flenner, I. Greving, M. Burger, C.G. Schroer and J. Hagemann

145. Advancing Time-Resolved X-ray Techniques at PAL-XFEL FXL: Instrumentation and Science Highlights
R. Ma, J. Hyuk Lee and Y. Kim

146. Recent Progress of the Biological Research Platform at PAL-XFEL
J. Park, S.J. Lee, S. Park, S. Chun and I. Eom

EKSMA OPTICS

Your reliable partner for
PHOTONICS INNOVATIONS

Laser Optics & Electro-Optics Tailored for High Performance

IBS Coated Optical Components (200-3000 nm)

Optical Assemblies Opto-Mechanics

Femtoline & Nd:YAG LaserLine

Nonlinear & Laser Crystals

EKSMA Optics is a manufacturer and global supplier of precision optics and optical assemblies, electro-optical and electronic components used in laser and other photonic instruments.
EKSMA Optics manufacturing capabilities include:

- Assembly of electro-optical and optical systems in cleanroom environment
- Advanced optical coating capabilities
- Polishing of a variety of optical and crystal materials
- Production of precision spherical, aspherical & conical lenses
- Optical, opto-mechanical design services and prototyping

We offer a wide range of standard catalog products for fast-off-the-shelf delivery, as well as custom-tailored optical components and assemblies optimized for your application-specific requirements.

TAKE A VIRTUAL TOUR

EKSMAOPTICS.COM

Design

Manufacturing

Fast delivery

---

iseg

HIGH VOLTAGE. EXACTLY.

SHR

ULTRA PRECISE HIGH VOLTAGE SOURCE+MEASURE UNIT

ELECTRONICALLY SWITCHABLE POLARITY

- High Voltage SMU (Source and Measure Unit)
- 4 channel output with up to 6 KV
- High-precision, very low ripple and noise
- 50 pA current measurement resolution

DESIGNED FOR UNIVERSAL LABORATORY USE

The SHR series represents standalone high precision, high voltage laboratory SMU - Source Measuring Unit - equipped with the finest iseg high voltage generation technology and iCS control system.

ISEG-HV.COM/SHR

147. Investigating the Ultrafast Molecular Relaxation of 4- Thiouracil Using Time-Resolved X-ray Photoelectron Spectroscopy
D. Mayer, D. Picconi, J. Pedersen, M. Bonanomi, M. Danailov, A. Demidovich, M. Devetta, M. di Fraia, D. Facciala, R. Feifel, C. Grazioli, F. Lever, N. Pal, V. Petropoulos, K. Prince, O. Plekan, R. Squibb, C. Vozzi, G. Cerullo, S. Coriani and M. Gühr

148. Insights into Cochleate Structures by Means of SAXS
P. Garidel and S. S. Funari

149. Mapping Molecular Photodynamics of CS_2 with Soft X-rays in Site-Selective Investigations
H.J. Thompson, M. Bonanomi, J. Pedersen, O. Plekan, N. Pal, C. Grazioli, K.C. Prince, B. N. C. Tenorio, M. Devetta, D. Faccialà, C. Vozzi, P. Piseri, M.B. Danailov, A. Demidovich, A.D. Brynes, A. Simoncig, M. Zangrando, M. Coreno, R. Feifel, R.J. Squibb, D.M.P. Holland, F. Allum, D. Rolles, P. Decleva, M.S. Schuurman, R. Forbes, S. Coriani, C. Callegari, M. Di Fraia and R. S. Minns

150. Smart*light: A New Inverse Compton Hard X-ray Source From The Netherlands
M. Alfeld, G. Welker, L.M. de Almeida Nieto, I. van Elk, C. Sweers, P.H.A. Mutsaers, O.J. Luiten and J. Dik

151. The Development and Application of Small-Rotative Fixed-Target Serial Synchrotron Crystallography (SR-FT-SSX) on I19
S. Lewis, M. Warren and L. Hatcher

152. AHP1 and ARR1 interaction in the multi-step phosphorelay system
L. H. Tran and M. Ruszkowski

153. Pair Beams Unlock Beyond Terawatt Attosecond Free-Electron Lasers
C. Erciyes, C. H. Keitel and M. Tamburini

154. Data-Driven Analysis of XRF and XEOL Spectra Using Neural Networks
M. Völschow, M. Stückelberger, N. Pyrlik, G. Falkenberger, T. Kaiser and P. Buczek

155. Advancement of FLASH effect for cancer therapy: Exploring the elementary processes of radiation chemistry induced by ultra-high dose rate
B. Sedmidubská, L. Vyšín and L. Juha

156. Biological applications at the AQUA beamline of the EuPRAXIA@ SPARC_LAB free electron laser
F. Stellato

157. Electric Field-Induced Lattice Strain Evolution in Perovskite Solar Cells
I.Y. Lee, S. Seo and H.J. Kim

158. High-throughput studies of multi-component thin films
D. Lapkin, G. Melis, A. Abukaev, R. Nasro, O. Konovalov, A. Hinderhofer and F. Schreiber

159. Modeling the effects of XFEL irradiation on photovoltaic materials
A. Artímez-Peña and N. Medvedev

160. XTANT-3: modelling irradiation of complex materials
N. Medvedev

161. Status and upgrades of the REGAE facility
V. Hennicke, M. Hachmann, S. Hayes, J. Meyer, T. Pakendorf, K. Floettmann and A. Meents

162. Do you dare to compress?
J. Hagemann and E. Weckert

163. A role of dihalides in solvation dynamics of nascent halides
Z. Nurekeyev, H. Hwang, M. Sekkal, K. Kubicek, C. Bressler, M. U. Reidelbach, M. Schneeberger, M. Bai, C. Herrmann, M. Thorwart, D. Fan, R. Haruki and S. Nozawa

164. Imaging the Electronic Performance of Semiconductor Devices in the Lab
R.Y. Engel, E. Ametova, S. Hampel, S. Patjens, J.L.J. Barp and M.E. Stuckelberger

165. Correlation analysis of hydrogen-induced blistering and structural characteristics in Mo/Si multilayers for EUV blank masks
Y. J. Kim, I. H. Cho, H. H. Lee, K. H. Jo and H. J. Kim

166. Transient Current Characterization of an Asymmetric p–i–p Diode for XFEL Applications
M. Sarajlic, S.D. Ilic, G. Kramberger and B. Hiti

167. Recent developments in diffractive and refractive X-ray optics
A. Kubec, J. Erjawetz, D. Eschimese, J. Gutekunst and F. Döring

168. snip – user centric collaborative ELN
S.B. Mohr and M. Osterhoff

169. OSCARS enhancing the applications of PaNET
M. Nentwich, P. Fuhrmann, A.P. Millar and H. Mohamed

170. Ultrafast radiation chemistry of glycine in aqueous solution
M. Goullieux, A. Ferté, A. Martinez Gutierrez, L. Inhester and R. Santra

171. Numerical Foot-print Correction Methodology for X-ray Reflectivity
T. Matar, W. Corts, S. Tober, P. Walter and H.-G. Steinrück

172. X-ray in-operando characterization to advance sustainable material development
L. Zorzetto, O. Späker and W. Wagermaier

173. Structural basis for NanoLuc luciferase action
M. Marek

174. Exploring the Response of Liquids to Ionizing Radiation with Ultrafast X rays and Simulations
L. Inhester

175. Tracking ultrafast changes of optical polarization in XUV irradiated diamond
S. Antunes, F. Capotondi, K.J. Kapcia, V. Lipp and B. Ziaja

176. Sequential insulator-metal-insulator transitions in photoexcited V_2O_3 films resolved by ultrafast X-ray Bragg diffraction
O. Gorobtsov, Y. Kalcheim, Z. Shao, A. Shabalin, N. Hua, D. Weinstock, R. Bouck, M. Seaberg, D. Zhu, O. Shpyrko, I. Schuller and A. Singer

177. Insights into Photocatalytic CO_2 Reduction on Zeolites Revealed by XFEL-Based Coherent X-ray Diffraction
J. Kang, J. Park, S. Ha, C. Kim, K. Ahn, S. Choi and S. Kim

178. Beams of shockfrozen and controlled nanoparticles and bio-macromolecules
J. He

179. Sample delivery of shockfrozen
K. Janson

180. Tunable, high-power deep UV to NIR source of femtosecond pulses utilizing various Yb-doped pump-laser architectures
P. Merkla, T. Braatza, M. J. Prandolinia, H. Goudarzia, S. Starosieleca, T. Golza, B. Manschwetusa, M. Schulza and R. Riedela

181. Functional characterisation of the luminous apparatus of the sea pen Pennatula phosphorea
M. Sitte, D. Pluskal, M. Sulova, L. Duchatelet, J. Damborsky, J. Delroisse and M. Marek

182. Polariton spectroscopy at the diamond K-edge via X-ray parametric down-conversion
F. Kerker, D. Krebs, X. Brockmüller, A. Negi, C. J. Sahle, B. Detlefs and C. Bömer

183. BEAMS for Industry
D. Sarabi, M. W. Larsson, S. Mufti, C. Lyons and L. Duregård

184. Sample delivery of shockfrozen nano-beakers for X-ray diffraction imaging and cryo-EM
M. Memovich and K. Janson

185. Imaging chemical dynamics
S. Trippel, A. Ayalsi, L. Blum, H. Bromberger, W. Jin, S. V. Makam, A. Pradhan, M. S. Robinson, M. Singh, N. Vadassery, I. S. Vinklárek and J. Küpper

186. X-ray parametric down-conversion reveals EUV-polariton
D. Krebs, F. Kerker, X. Brockmueller and C. Boemer

187. Observation of the crystallisation in 95 $V_2O_5 \cdot 5\ P_2O_5$ glass in in-situ XAS measurements.
K. Gadomski, M. Jankowska, W.Tabiś, G. Gazdowicz, A. Maximenko, S. J. Rzoska and T. K. Pietrzak

188. Non-equilibrium Dynamics of Water Ingress into Sodium Bentonite
R.P.C. Bauer, W. Roseker, Q. Zhang, G. Hinsley, S. Narayanan, T. Nagel and F. Lehmkühler

189. The Helmholtz Model Zoo: Enabling AI Model Sharing and Inference in the Helmholtz Cloud
H. Werners, E. Eren and P. Heuser

190. Imaging aerosolized PR772 viruses using an XFEL
T. B. Berberich and R. P. Kurta

191. Application of Synchrotron Radiation Technology in Perovskite Solar Cells
W. Hui and L. Song

II.4 PETRA III

192. Study of multiphase indium nanoparticles, self-organized on the surface and in the bulk of the organic matrix CuPcF4: morphology and electronic properties of the nanocomposite material.
O.V. Molodtsova, D.V. Potorochin, A.N. Chaika, S.V. Babenkov, S.L. Molodtsov, A.A. Makarova, D.A. Smirnov and V.Y. Aristov

193. Modification of the electronic structure and morphology of few-layer graphene by functionalization with organic dyes using a diazonium chemistry approach.
V.Y. Aristov, D.V. Potorochin, O.V. Molodtsova, A.N. Chaika, D. Marchenko, A. Ciobanu, B. Walls and and S.L. Molodtsov

194. Beamline station P61B: X-ray Diffraction and Imaging at Extreme Conditions using the Large Volume Press
R. Farla, S. Bhat, K. Spektor, X. Feng, A. Neri, L. Man, A. Chanyshev, S. Sonntag, U. Haeussermann and T. Katsura

195. Streamlining Bio-Medical Tomography at GINIX
M. Osterhoff, J. Lucht, P. Meyer, J. Alfken and T. Salditt

196. Effects of perfluorocarbons on lipid monolayers and protein adsorption
J. Savelkouls, M. Paulus, C. Thiering, M. Dargasz, L. Friedrich, M. George, P. Hitaishi, S. Hövelmann, O. Konovalov, E. Schneider, G. Scholz, C. Shen and M. Tolan

197. Anomalous Thermal Evolution of Luminescent Properties in Sol–Gel Synthesized $LaAlO_3$ Nanoparticles and Their Suitability for Optical Thermometry
O. Chukova, I. Fesych and A. Kotlov

198. Engineering of spectral properties of ZnO nanoparticles in polymer media
O. Chukova, I. Fesych, T. Voitenko, L. Jacobsohn and A. Kotlov

199. Axicon elements for Full-field TXM
J. Vila-Comamala, A. Bonnin, I. Greving, P. Qi, H.-Y. Cheng and S. Flenner

200. GaAs Waveguides for Hard X-ray Imaging
I. Zamboti, M. Kanbach and T. Salditt

201. High-background X-ray single particle imaging enabled by holographic enhancement with 2D crystals
A. Mall, Z. Shen and K. Ayyer

202. ASAPO framework for real-time data analysis
M. Karnevskiy

203. Holstein Polaron Formation in the semimetallic mixed-valent $TmSe_{1-x}Te_x$ system
C.-H. Min, S. Müller, W. J. Choi, L. Dudy, M. Heber, J. D. Denlinger, C.-J. Kang, M. Kalläne, N. Wind, M. Scholz, C. Schlueter, A. Gloskovskii, H. Bentmann, Y. S. Kwon, F. Reinert, H.-D. Kim and K. Rossnagel

204. Biopolymer-Templated Deposition of Hierarchical 3D-Structured Graphene Oxide/Gold Nanoparticle Hybrids for Surface-Enhanced Raman Scattering
Y. Guo, G. Pan, Yusuf Bulut, A. Jeromin, T. F. Keller, A. Stierle, G. Nemeth, F. Borondics, B. Sochor, S. K. Vayalil, D. Söderberg, P. Müller-Buschbaum and S. V. Roth

205. Understanding precipitation reactions for phosphorus recovery from wastewater.
H. Akhtar, P. Hausbrandt, T. Hochdörffer, M. Hoock, V. Christl, X. Mechler and V. Schünemann

206. Ligand-Controlled Fluorescence in Square-Planar Nickel(II) Phenazine Complexes: Exploring Photo-Excited State Dynamics
H. Hwang, F. Rodriguez Diaz, Z. Nurekeyev, K. Kubicek, G. Hörner, F. Daumann, H. Kurz, A. Jha, A. Bailie, S. Botchway, B. Weber and C. Bressler

207. X-ray photon correlation spectroscopy of hydrated lysozyme at elevated pressures
M. Åhlfeldt, M. Bin, A. Girelli, I. Andronis, A. Karina, N. Das Anthuparambil, F. Berner, T. Eklund, L. E. Kraft, A. Leonau, F. Westermeier, M. Sprung, C. Gutt, K. Amann-Winkel and F. Perakis

208. CoRDIA: a >100kHz, continuous imaging detector
A. Marras

209. Multifunctional X-ray study on thulium doped Al2O3 thin films for photonic applications
K. Schlage, J. Lorenzen, S. Velten and N.L. Colomer

210. New possibilities of the Langmuir trough GID setup at P08 for characterizing liquid surfaces.
C. Shen

211. The P66 beamline status
A. Kotlov, Y. Smortsova, O. Chukova and A. Kataev

212. High-flux, High-Z sensors characterization at P07-B
D. Magalhaes, M. Ruat, A. Rothkirch, O. Gutowski, T. Laurus, J. Schwandt, S. Martens, H. Hirsemann, S. Lange, M. Niemann, M. Hajheidari, A. Klujev, M. Veale, N. Schell, E. Garutti, H. Graafsma

213. Towards in-operando investigations of pigment degradation processes
E. Avranovich Clerici, F. Broers, R. Oord, S. Carboni Marri, B. den Hartigh, A. Gestels, A. Marchetti, G. Nuyts, L. Monico, F. Vanmeert, J. Garrevoet, M. Alfeld, K. Keune, F. Meirer, G. Falkenberg and K. Janssens

214. Strain mapping of martensitic steel crack tips studied with μ-XRD and XRF imaging
A. Khaliq, F. Wittwer and P. Modregger

215. X-ray holo-tomography reveals 3D structure of protein networks and lipid globules in heat-treated egg yolk
F. Wittwer, N. D. Anthuparambil, F. Unger, R. P. Gautam, S. Flenner, I. Greving, C. Gutt and P. Modregger

216. Antimony isotope fractionation in hydrothermal systems – In need of support by synchrotron-based spectroscopic techniques
J. Majzlan

217. Revealing time-resolved structure formation in biohybrid coatings using in-situ GISAXS and machine learning
J.E. Heger, S. Dan, Y. Zhai, S.V. Roth and P. Müller-Buschbaum

218. Real-Time GIWAXS Investigation of Structural Evolution in All-Solid-State Lithium Batteries
Y. Liang, K. Sun, T. Guan, Y. Yan, F.A.C. Apfelbeck, Y. Cheng, M. Schwartzkopf, S.V. Roth, S. Koyiloth Vayalil and P. Müller-Buschbaum

219. PETRA III Experiments - Brilliant opportunities for Photon Science
H.-C. Wille, O.H. Seeck and C. Schroer

220. TEMPUS, a Timepix4-based event driven detector for Photon Science
J. Correa, A. Simancas, D. Pennicard, S. Fridman, S. Lange and H. Graafsma

221. P03 - A flexible X-ray scattering beamline of PETRA III for studying nanostructure dynamics under in situ/ operando conditions
J. Rubeck, A. Chumakov, J. Neumann, V.N. Manoj Kumar, A. Davydok, C. Krywka, M. Schwartzkopf and S. Koyiloth Vayalil

222. Deciphering the photopolymerization-induced nanostructure and interface formation for submicron additive manufacturing
S. Chen, Y. Zhai, J. Zhou, L. Li, J. Jansen, R. van Benthem, M. Johansson, P. Müller-Buschbaum and S.V. Roth

223. Molecular Brushes with Poly(2-oxazoline)-based Amphiphilic Diblock Copolymer Side Arms
W. Xu, L. Fietzke, R.A. Gumerov, F. Zheng, P. Zhang, C. Jeffries, I.I. Potemkin, R. Jordan and C.M. Papadakis

224. Probe-informed phase retrieval for X-ray phase contrast tomography
J. Lucht, Y. Rossi-Tonin, C. v. Carnap, P. Meyer, A. Wald and T. Salditt

225. HoToPy: a toolbox for X-ray holo-tomography in Python
J. Lucht, P. Meyer, L. M. Lohse and T. Salditt

226. 2D-PDF data reduction: for fibre textured (thin film) samples with ID #73 has been accepted in track
J. Liu, A.-C. Dippel and M. von Zimmerman

227. X-ray fluorescence imaging for in vivo localization of therapeutics
M.M. Bidhendi, L. Dalipi and S.C. Fedosejevs

228. Nuclear inelastic scattering of a molecular single crystal at 10 K
M.A.M. Tummeley, J.A. Wolny, T. Hunsicker, K. Gröpl, T. Hochdörffer, D. Prajapat, I. Sergeev and V. Schünemann

229. New Soller slits instrumentation at P02.2, PETRA III, DESY for total X-ray scattering measurements of disordered materials at extreme conditions
C. Otzen, G. Cocomazzi, A. Phelipeau, M. Wendt, K. Glazyrin, H.-P. Liermann and C. Prescher

230. Near-field Hologram Denoising Using Dilated Convolutional Neural Networks
V. Rahmani, J. Hagemann and C.G. Schroer

231. Operando X-ray Scattering during Laser Reactive Sintering of Nanoparticle Films
J. Schulte, M. Winterer and M.A. Schroer

232. P25: Beamline for Applied Bio-Medical Imaging, Powder Diffraction and Innovation
K. Spiers, N. Thielen, C. Qiu, S. Hampel, N. Samadi, M. Etter, A. Schoekel, V. Baran, A. Burkhardt, G. Falkenberg and H.-C. Wille

233. Fragment Based Active Site Exploration of Plastic Degrading Enzymes at Ambient and Cryogenic Temperatures
D. Bicer, L. Rotilio, S. Thirup, D. Otzen and J. Morth

234. The High-Resolution Diffraction Beamline P08
F. Bertram, R. Kirchhof, C. Shen and P. Saha

235. Morphological Insights into Spray-Coated Organic Semiconductors
S. Xiong, M. Betker, S. Schraad, Y. Zhai, B. Sochor, S. Koyiloth Vayalil, P. Müller-Buschbaum and S.V. Roth

236. Mass Spectrometry for Single Particle Imaging of Dipole Oriented Complexes (MS SPIDOC) and First Scattering Measurements of Gas-phase Protein Complexes
J.C.K. Kung, T. Damjanovic, S. Mishra, T. Kierspel and C. Uetrecht

237. EXAFS Spectroscopy of WO_3 Nanoparticles Combined with Reverse Monte Carlo Modeling
V. Dimitrijevs, A. Kuzmin and E. Welter

238. From gas-phase to liquid phase: probing the electronic structure of amino acids with X-ray spectroscopy
J. Leroux, N. Velasquez, J.-Y. Chesnel, A. Nair, B. Oostenrijk, C. Mahecha, F. Trinter, L. Pille, M. Ilchen, L. Schwob and S. Bari

239. In situ X-ray probing of nanoparticle formation in Chemical Vapor Synthesis
S.R. Joshi, M.A. Schroer and M. Winterer

240. X-ray spectroscopy meets native mass spectrometry: probing gas-phase protein complexes
S. Mishra, T. Kierspel, J. Kung, T. Damjanović and C. Uetrecht

241. Atomic-Scale Evidence of Local Distortions in (MgCoNiCuZn)O High-Entropy Oxide
J. Lukasevica, A. Kuzmin and E. Welter

242. The DESY Beamline Agent
S. Singh, L. Pithan and P. Heuser

243. 10 years of Biological Small-Angle Scattering Data Curation - SASBDB
A. Sutinen, C. Blanchet, M. Graewert, D. Soloviov and T. Tropin

244. Machine Learning in the Study of Pinealocytes in Aging and Alzheimer's Disease
I. Bukreeva, O. Junemann, F. Palermo, M. Fratini, S.V. Saveliev and A. Cedola

245. Tracking carbon-induced atomic scale effects in (CrMnFeCoNi)1-xCx HEAs via multi-edge EXAFS spectroscopy and DFT simulations
A. Smekhova, A. Kuzmin, G. M. Muralikrishna, E. Welter, S. Levcenko, F. Körmann, Y. Ikeda and S. V. Divinski

246. Operando characterisation of Cu-based catalysts for DME steam reforming
S. Tober, N. Heiming, M. Battisti, S. Benjamaa, T. Duyster, A. Eshesheva, F. Igoa, A. Khadiev, A. Mijovilovich, J. Ruello, N. Simitsis, F. Sit, T. Weigel, C. Asmelash and H.-G. Steinrück

247. Simultaneous in operando synchrotron XRD and interferometric expansion study of a commercial Lithium Iron Phosphate cell under varying load profiles
S. Gielinger, S. Breitfelder, T. Staab and G. Bohn

248. In-situ USAXS and XPCS Investigation of the Structural and Dynamic Evolution of Corn Starch Gels under Ionic Influence
A. M. Raza, N. Anthuparambil, F. Unger, A. Tosson, A. Leonau, M. Dargasz, R. Gautam, X. Liu, M. Puritscher, F. Zhang, F. Westermeier, F. Schreiber and C. Gutt

249. Atomistic Approach to Thermal Disorder in HCP Zinc
V. Dimitrijevs, I. Pudza, P. Žguns, A. Kalinko and A. Kuzmin

250. Structural Investigation of the Alkyltransferase Ribozyme SAMURI
H.-A. Chen, T. Okuda, A.-K. Lenz, C. Scheitl, H. Schindelin and C. Höbartner

251. Probing the Oxide Interface Structure under Reaction Conditions by Operando Surface X-ray Diffraction
C.H. Scharf, A. Chandraraj, K. Dyk, F. Stebner, S. Lepin, J. Tian, L. El Bergmi Byaz, J. Stettner, C. Leppin, A. Kotova, S. Reinke, Catalina Leiva-Leroy, J. Linnemann, M. Muhler, F. Maroun and O.M. Magnussen

252. Combined Holotomography Reconstruction: Joint Phase Retrieval and Tomography.
D. H. Duran, J. Dora, J. Hagemann, C. Schroer and T. Knopp.

253. Investigation of Structural Heterogeneity in Soft Magnetic Materials Formed by Hot Powder Compaction
J. Bednarcik, P. Dubecky, J. Drahokoupil, K. Kosiba and P. Kollar

254. Grain Size Determination using XRD Line Profiles via Iterative Convolution
P. Dubecky, R. Kaur, P. Sovak and J. Bednarcik

255. First look at a new 14.5 GHz ECR Ion Source
M. Tatsch, M. Döhring, K. Huber and S. Schippers

256. Light excited states of iron spin crossover systems and electronic properties of iridium complexes explored by nuclear resonance scattering
K. Gröpl, T. Hunsicker, J. A. Wolny, M. A. M. Tummeley, T. Hochdörffer, H. Akhtar, D. Prajapat, I. Sergeev, M. H. Hoock, J.-G. Becker, E. Rentschler and V. Schünemann

257. Beamline P61A, Engineering Materials Science with a white beam at PETRA III
G.A. Faria

258. The lattice parameter development of Zinc (Zn), during fast compression in the dDAC.
C. Plueckthun, J. M. Kaa, N. Giordano, R. Husband, M. O. Schoelmerich, S. Merkel, R. Redmer and Z. Konopkova

259. Everybody likes it multi-modal and operando! Simultaneous photoemission and structural measurements of gas–solid catalysts under 1 bar at beamline P22
F. Garcia-Martinez, W. Corts, S. Tober, M. Beye, H.-G. Steinruck and C. Schlueter

260. Spatially-resolved X-ray diffraction from perovskite supercrystals
J. Hiller, R. Thalwitzer, A. Bozkurt, R. Carter, T. Hettiger, M. Fröhlich, R. Hodak, M. Ferreira, M. Eberle, E. Kneschaurek, G. Hinsley, B. Wang, K. H. Ngoi, E. Nadler, W. Roseker, F. Westermeier, M. Sprung, D. Baranov, J. Lauth, F. Schreiber, I. Vartanyants, M. Scheele and I. Zaluzhnyy

261. Generic Rolling Access at five PETRA III beamlines (P08, P11, P22, P23, & P24)
A.B. Dey, K. Bagschik, J.-P. Kurz, D. Unger, F. Bertram, J. Hakanpää, C. Schlueter, D. Novikov, M. Tolkiehn, M. Lippmann, L. Noohinejad, H.-C. Wille, O. H. Seeck and H. Reichert

262. Concept of Generic Rolling Access
A.B. Dey, K. Bagschik, J.-P. Kurz, D. Unger, F. Bertram, J. Hakanpää, C. Schlueter, D. Novikov, M. Tolkiehn, M. Lippmann, L. Noohinejad, H.-C. Wille, O.H. Seeck and H. Reichert

263. mlgid – Machine Learning for Grazing-Incidence Diffraction (GID): from Raw Data to Crystalline Structure
D. Lapkin, A. Abukaev, E. Kneschaurek, V. Munteanu, M. Romodin, C. Völter, E. Pfeiler, I. Zaluzhnyy, C. Shen, F. Bertram, O. Konovalov, V. Starostin, L. Pithan, M. Jankowski, W. de Nolf, S. Kowarik, A. Hinderhofer and F. Schreiber

264. Morphometric Analysis for 3D Histopathology of Duchenne Muscular Dystrophy
S. Becker, J. Alfken, E. Haupt, R. Scodellaro, F. Alves, J. Zschüntzsch and T. Salditt

265. Biological SAXS on the P12
D. Soloviov, M. Graewert, A Sutinen, T. Tropin and C. Blanchet

266. High-Spatial Resolution Full-Field XANES Tomography at Beamline P64, PETRA III
S. Alizadehfanaloo, D.E. Doronkin and A. Kalinko

267. Correlation of nanoscale structure, composition, and performance: a study of the CIGS Materials Paradigm
N. Pyrlik, C. Ossig, S. Patjens, G. Fevola, J. Hense, C. Ziska, M. Seyrich, F. Seiboth, A. Schropp, J. Garrevoet, G. Falkenberg, C. G. Schroer, R. Carron and M. E. Stuckelberger

268. Latex film formation investigated by GISAXS
S. Schraad, S. Xiong, H. M. Salvador, P. Müller-Buschbaum and S.V. Roth

269. AXOLOTL 2.0: Analyzer of X-ray excited optical luminescence (XEOL) offering temporal and spectral resolution for scanning X-ray microscopy
G. Falkenberg, J. L. Barp Jr. and C. Osssig, S. Patjens, S. Hampel, N. Pyrlik, G. Fevola, C. Strelow, T. Kipp, J. Garrevoet, G. Falkenberg, C. G. Schroer and M. E. Stückelberger

270. Powder Diffraction Under Pressure - A new Hydrostatic Pressure Diffraction Cell
L. Sippach, H. Geraissate, A. Meyer, A. Schoekel, A. Ehnes and G. Kieslich

271. Investigation of the LOHC's Dehydrogenation Dynamics via Simultaneous SAXS/WAXS
F. Şit, J. Yoo, A. Kuhlmann, T. Duyster, A. Saleev, T. Sharma and H. G. Steinrück

272. Deep Learning for 3D Integrated Circuits inspection.
A. Karabay, A. Khorashadizadeh, M. Guizar-Sicairos, I. Greving, S. Flenner, P. Paetzold, J. Kim, L. Barba, J. Kirschner, M. Holler, T. Aidukas, E. Muller, S. Stutz, T. Levi and W. Unglaub

273. Epitaxial Strain Stabilizes Ferroelectric SnSe in the Monolayer Limit
D. Wilks, V. Vonk, P. Aleksa, S. Chung, A. Bremerich, T. Chagas, D. V. Novikov, P. Modregger, A. Stierle and C. Busse

274. Improvements in Implicit Neural Representations for Holotomography
S. Eberle, J. Gruen, I. Greving, S. Flenner, M. Burger, C. G. Schroer and J. Hagemann

275. Studying Structural Transformations of Catalysts inside Reactors by Iso-Potential Operando X-ray Diffraction at a Synchrotron and a Laboratory Diffractometer
G. Gizer, H. M. Zeeshan, H. Appala, K. C. Bharatula, B. Wollak, F. Igoa, P. Glaevecke, A. Dippel, O. Korup, M. Schmidt and R. Horn

276. In situ X-ray studies reveal the formation mechanism of crumpled iron sulfide nanosheets
C. Zito, L. Klemeyer, F. Caddeo, Brian Jessen, S. Y. Harouna-Mayer, A.-C. Dippel, F. Igoa Saldaña and D. Koziej

277. Room-temperature X-ray fragment screening with serial crystallography
S. Guenther, P. Fischer, M. Galchenkova, S. Falke, P.Y.A. Reinke, S. Thekku Veedu, A.C. Rodrigues, J. Senst, D. Elinjikkal, L. Gumprecht, J. Meyer, H.N. Chapman, M. Barthelmess and A. Meents

278. Studying Structural Transformations of Catalysts inside Reactors by Iso-Potential Operando X-ray Diffraction at a Synchrotron and a Laboratory Diffractometer
G. Gizer, H. M. Zeeshan, H. Appala, K. C. Bharatula, B. Wollak, F. Igoa, P. Glaevecke, A. C. Dippel, O. Korup, M. Schmidt and R. Horn

279. Resonant X-ray diffraction studies of $LiMn_2O_4$ epitaxial thin film
A. Benediktovitch, O. Yefanov, A. Dohn, M. Wachter-Lehn, M. Haubro, T.-K. Choi, D. Ronchetti, D. Alsamarraie, R. Meißner, G. Vonbun-Feldbauer, PETRA III-P23-team, EuXFEL-FXE-team, C. Milne, R. Pandya and N. Rohringer

280. Implementing a new detector for momentum resolved ionic molecular photo fragment detection
F. Junker, S. Reinwardt, A. Andreeva, A. Müller, S. Schippers, F. Trinter and M. Martins

281. Sample Preparation for Hybrid SERS Sensors
F. Gaede, Y. Zhai, S. Schraad, Y. Guo, T. Laarmann, P. Müller-Buschbaum and S. V. Roth

282. Molecular formation induced by soft X-ray irradiation in CH_4-N_2 gas mixtures
T. Proch, S. Reinwardt, J. Schwarz, A. Andreeva, M. Martins, A. Müller and S. Schippers

283. Physics-Informed Deep Learning for Thin-Film GISAXS Inversion
Ö.E. Aşırım, Y. Zhai, S.V. Roth and M. Tropmann-Frick

284. Bragg coherent X-ray diffraction imaging at P10 beamline, PETRA III
W. Roseker, G. Hinsley, D. Weschke and F. Westermeier

285. Status & New Developments at the Extreme Conditions Beamline (ECB, P02.2) PETRA III, DESY.
H.-P. Liermann, K. Glazyrin, N. Giordano, H. Frraj, B. Wang, E. Ehrenreich-Petersen, E. O'Bannon, M. Wendt, S. Wenz, A. Ehnes, I. Schwark, J. T. Roeh, C. Otzen and C. Prescher

286. Present and Future Extreme Conditions Research at Low (PETRA III) & Ultra-Low (PETRA IV) Emittance Synchrotron Sources at DESY.
H. P. Liermann and K. Glazyrin

287. AI-assisted catalytic metadata organiser for SciCat
A.Sapronov, A.Zimina and J.-D. Grunwaldt

288. Coherence Applications Beamline P10
F. Westermeier, N.D. Anthuparambil, G. Hinsley, V. Kartik, P. Middendorf, W. Roseker, A. Saleev, F. Unger and D. Weschke

289. Coherent X-ray Imaging of Skyrmion Motion in a Fe2GeTe3 van der Waals ferromagnet near Critical Temperature
S. Wagner, C. Klose, L. Randolph, H. Sun, D. Metternich, M. Schneider, J. Fuchs, M. Kamm, M. Hoesch, S. Chowdhury, C. Sharma, V. Deinhart, C. Gutt, B. Pfau and S. Eisebitt

290. Exploring the Mysteries of Melting: X-ray Diffraction Meets Phase-Contrast Imaging
E. Ehrenreich-Petersen, O. S. Pardo, T. Engler, B. Massani, K. Glazyrin, N. Giordano, J. Hagemann, M. Wendt, S. Wenz, C. G. Schroer, R. S. McWilliams, H.-P. Liermann, Zs. Jenei and E. F. O'Bannon

291. Clathrate formation from a supercooled liquid
A. Gierke, R. P. C. Bauer, C. Goy, E. Becquevort, J. Valerio, L. Adriano, S. Kang, M. Blankenburg, S. Gutschmidt, M. Walther, J. Schulz and F. Lehmkühler

292. 3D multiscale characterization of resected human hippocampal tissue using X-ray Phase-Contrast Tomography and quantitative MRI
N. Lüthi, J. Carstens, F. J. Fritz, N. Sura, C. Chavarrias, T. Sauvigny, N. Shemesh, T. Salditt and S. Mohammadi

293. Automated Reflectivity Analysis with AI: A FAIR Data Pipeline at P08
J. Kobus, N. Hayen, P. Jordt, A. Ashtiani, O. Lipmann, A. Hinderhofer, V. Starostin, V. Munteanu, P. Tirumalai, C. Shen, F. Bertram, W. De Nolf, J. Kotanski, L. Pithan, F. Schreiber and B. Murphy

294. SAS methods for the study of magnetic fluids and their composites ie transformer oil based MFs and textiles as examples
P. Kopcansky, M.Timko, M. Rajnakand I Safarik, V. Petrenko and O. Tomcuk

295. Deep Learning-Driven Grazing Incidence Small-Angle X-ray Scattering Data Processing for Nanostructure Characterization
Y.F. Zhai, J.G. Zhou, S. Dan, J. E. Heger, B. Sochor, A. Jeromin, W. Wang, W. J. Parak, S. Koyioth Vayalil, T.F. Keller, A. Stierle, A. Hexemer, P. Müller-Buschbaum and and S.V. Roth

296. The year 2025 at P06, PETRA III, an overview.
J. Garrevoet, K. V. Falch, D. Brueckner, S. Wenz and G. Falkenberg

297. Ultrafast dissociation dynamics of HCO^+
A. Andreeva, S. Reinwardt, J. Schwarz, B. M. Döhring, M. Tatsch, D. Macaluso, A. Müller, N. Solem, R. Thissen, F. Trinter, S. Schippers and M. Martins

298. How rapid quenching and heating cycles influence phase transformations in advanced gamma-TiAl alloys
A. Stark, M. W. Rackel and F. Pyczak

299. Analysis of Selected Samples of the Clemens-WinklerCollection of Historic Inorganic Specimens
G. Franze, M. Herbig, A. Rogoll, H. Schmidt, U. Lienert and E. Kroke

300. Advanced Structural Characterization of Ferroelectric AlScN/GaN Heterostructures by Coherent X-ray Diffraction Imaging and Nanofocused XRD
E. Dieball, N. Hayen, O. Lippmann, P. Jordt, F. Westermeier, L. Kienle, N. Wolff and B. Murphy

301. Advanced Analysis of 2D WS_2 X-ray Absorption Spectra via Reverse Monte Carlo and Molecular Dynamics Simulations
I. Pudza, P. Žguns, E. Welter and A. Kuzmin

302. Macromolecular Crystallography at Beamline P11.
A. Grebentsov, S.D. Chatziefthymiou, A. Gruzinov, O. Merkulova, G. Pompidor and J. Hakanpää

303. X-ray lens cubes with integrated aberration compensation
W. Wang, R. Döhrmann, S. Botta, A. Madsen, C. G. Schroer and F. Seiboth

304. Towards Near Real-time Computation of Autocorrelation Functions for X-ray Photon Correlation Spectroscopy using FPGAs
A. Saleev, P. Middendorf, F. Westermeier, R. Lammert, A. R. Tareen, C. Plessl, T. Kenter, H. G. Steinrück and C. Gutt

305. Visualization of stereo ptychography data using virtual reality tools
S. Sepanlou, A. Schropp, F. Steinicke and C. Schroer

306. Swedish Materials Science Beamline (SMS) at PETRA III: In-line branch (P21.2).
U. Lienert, S. Gutschmidt, Z. Hegedues, M. Blankenburg, N. Lefeld and H.H. Koenig

307. Investigation of effects of hydrodynamic interaction on protein dynamics at sub-zero temperatures using XPCS
R. Gautam, F. Unger, N. Anthuparambil, M. Dargasz, M. Raza, L. Randolph, E. Aydinlik, M. Rajan, W. Roseker, F. Westermeier, F. Lehmkühler and C. Gutt

308. Directional Dark Field for Nanoscale Full-Field Transmission X-ray Microscopy
S. Wirtensohn, S. Flenner, D. John, P. Qi, C. David, M. May, P. Huber, D. Herzog, S. Tangl, C. Kampleitner, K. Singh, I. Kelbassa, K. Bekes, J. Herzen and I. Greving

309. Imaging magnetic domains with hard X-ray full-field nano-imaging at P05
T. Scherbacher, I. Greving, D. Lott and S. Francoual

310. Progress in Liquid Jet Photoemission Spectroscopy at P04
F. Trinter, D. Stemer, H. Kaur, M. Pugini, Q. Zhou, N. Velasquez, L. Tomaník, M. Marraci, N. Iurgenson, E. Rouquet, S. Thürmer, U. Hergenhahn and B. Winter

311. Visualization of Phase Modulation in Ptychographic Imaging Near the Bragg Condition
C. Sow, M. Seyrich, F. Wittwer, J. Garrevoet, K. V. Falch, T. Diem, T. F. Keller, C. Schroer and A. Schropp

312. X-ray diffraction probing the molecular contraction machinery of living heart muscle cells
H. Bruns, M. Dvořák, K. Vu, T. Czajka, A. Conceição, M. Osterhoff, S. Brandenburg, T. Salditt

313. Observing nanoscale dynamics of living engineered heart muscle tissue using X-ray diffraction
M. Dvořák, H. Bruns, T. Czajka, M. Osterhoff, G. Dittrich, A. Conceição and T. Salditt

314. Combined XAS and XRD studies of $CuO/ZnO/Al_2O_3$ spinel-type catalysts for DME steam reforming
A. Eshesheva, N. Heiming, S. Tober, T. Weigel, M. Battisti, A. Mijovilovich, A. Khadiev, C. Asmelash and H.-G. Steinrück

Clean room technology for any workplace in industry and research!

Series SuSi Super Silent

Clean room station CleanBoy®
- Clean room conditions ISO 5
- Low investment costs
- Table-top or floor standing device
- Simple to set up

Clean room cell
- Clean room class A–D or ISO class 5–8
- Modular
- Flexible
- Freely selectable size

www.spetec.de

Spetec GmbH
Am Kletthamer Feld 15
D-85435 Erding

Tel. + 49 8122 95909-0
Fax: + 49 8122 95909-55
Email: spetec@spetec.de

315. 3D virtual histology investigation of ductal carcinoma in situ
G. Saccomano, M. Ackermann and T. Salditt

316. Characterization of metal hydrides using X-ray nanotomography imaging
S. Sefa, F. Karimi, I. Greving and C. Pistidda

317. In situ studies of $\delta - \gamma$ phase competition and transformations in Fe-Co-based alloys
S. Liu, V. Kaban, O. Gutowski and I. Kaban

318. Full-field Nanotomography at high time resolution, for in-situ, high throughput and multi-modal applications
I. Greving, S Wirtensohn, S. Sefa, T. Scherbacher, J. Hagemann and S. Flenner

319. Operando Profiling of Industrial Catalysts by Simultaneous X-ray Diffraction Tomography with Intrapellet Species Concentration Profiles
H. Appala, K. Ishakova, O. Gutowski, M. Finkeldei, T.L. Sheppard, O. Korup and R. Horn

320. Electron Bunch and Laser Pulse Dynamics in an Inhomogeneous Plasma Channel at Laser–Plasma Acceleration for PETRA IV
V.I. Maslov, N. Mykhailyshyn, D.S. Bondar, W.P. Leemans and M. Seniak

321. Depth resolved Structural studies in HM/FM/HM and HM/FM/MgO multilayers using x ray waveguide.
M. Singh, A. Gloskovsky, C. Meneghini, S. Francoual, Dmitri, I. Carlomagno, P. Gupta, M. Gupta, S. Pathak, S. Koyiloth Vayalil and A. Gupta.

322. ENCI Portable CT Scanning in the Field: Archaeological Objects from Museums in Ankara and Kayseri
S. Ehteram, P. Paetzold, A. Schropp, A. Beckert, R. Döhrmann, P. Wiljes, M. Bohn, A. Aksoy, S. Olbrich, C. Michel and C. Schroer

323. Development and Commissioning of Bluesky and Gas Dosing System for In-Situ Catalysis at P65 : ROCK IT
A. Bhogra, D. Burke, Z. I. Isik Dursun, S. Ehab, A. Naja, M. M. Kazemi, S. Levcenco, L. Pithan, A. Schökel, U. Singh, E. Weckert and E. Welter on behalf of the ROCK-IT Team at Deutsches Elektronen-Synchrotron DESY.

324. Dual-Site Mg2+ Substitution in LaFeO3 Ceramics: Defect Engineering and Multifunctional Property Modulation
S. Nandy, S. Ghosh, V. Samanta, M. Theingi, K. Hwa Chae and S. Chandran

325. Coherence and Phase Contrast in Synchrotron and Laboratory Full-Field Imaging
J.Carstens and T.Salditt

326. Experimental possibilities at the In-Situ X-ray Diffraction and Imaging Beamline at PETRA III
A. Khadiev, S. Tober, Y. Matveev, M. Hoffman, F. Bertram and D. Novikov

327. Mixed-contrast for X-ray near-field holography: A study of conditions influencing reconstruction quality of absorption values
J. Dora, C. G. Schroer and J. Hagemann

328. Centre for Molecular Water Science (CMWS)
C. Goy, M. Ayon Alfaro, F. Lehmkuehler, P. Huber and M. Schnell

329. Capillary-based Soft X-ray Ptychography for Ultimate 4D Spectro-Microscopy with Versatile Sample Environment
B. Sorokin, M. Raboni Ferreira, R. Khubbutdinov, K. Litzius, K. Bagschik, M. Hoesch, C. Donnelly, B. Pfau and F. Buettner

330. Pt-based Catalysts for NOx Reduction in Exhaust Gas: The Role of Tungsten and Molybdenum Additives
Z. Borowska, Ö. Selcuk, R. Schoch, S. Kureti, F. Fischer and M. Bauer

331. Measurement of beam vibrations at PETRA III beamlines P09, P23 and P62
M. Seyrich and J. Raabe

332. DataDOIs with SciCat at DESY
A. Aggarwal, R. Hinzmann, N. Hayen and L. Pithan

333. Exploring the 3D Structure, Connectivity and Integrity of Microchips
P. Paetzold, A. Schropp and C.G. Schroer

334. Automated sample handling for operando catalysis at synchrotron facilities
S. Ehab on behalf P65 and the ROCK-IT team

335. Deciphering brain tumor pathology in a new dimension
J. Alfken, S. Becker, Y. Schumann, J. Ahrens, C. Schroer, P. Neumann, M. Glatzel, T. Salditt and J.E. Neumann

II.5 Additional Posters

336. The Femtosecond X-ray Experiments (FXE) Instrument at the European XFEL
D.B. Jakobsen, F. Alves Lima, M. Biednov, P. Frankenberger, S. Hayes, X. Huang, S. Huynh, D. Khakhulin, M. Knoll, M. Othman, A. Sarkar, M. Sekkal, Y. Uemura, H. Wang, H. Xu, H. Yousef, P. Zalden and C. Milne

337. RefXAS – a curated database for X-ray absorption spectra with metadata and scientific quality control
A. Gaur, S. Paripsa, F. Förste, D. Doronkin, W. Malzer, C. Schlesiger, B. Kanngießer, D. Lützenkirchen-Hecht, E. Welter and J.-D. Grunwaldt

338. Time-Resolved X-ray Diffraction of THz-Induced Structural Dynamics in Solid State Electrolyte c-LLZO
M.T. Wachter-Lehn, A.O. Dohn, M.L. Haubro, C.J. Milne, F.A. Lima, K. Mitterer, H. Xu, H. Lemke, K. Haldrup, M.M. Nielsen and R. Pandya

III Author Index (Submitting author only)

(Submitting author and poster number)